

Geochemistry of Metapelite Hosted Tourmalinites, Eastern Alps, Austria

Richard Göd¹, Gerhard Heiss² & Friedrich Koller¹

11 Text-Figures, 4 Tables

Österreichische Karte 1:50.000
 Blatt 103 Kindberg
 Blatt 104 Müritzschlag
 Blatt 105 Neunkirchen
 Blatt 106 Aspang Markt
 Blatt 107 Mattersburg
 Blatt 134 Passail
 Blatt 135 Birkfeld
 Blatt 136 Hartberg
 Blatt 137 Oberwart

Boron metasomatism
 Grobgness Complex
 Lower Austroalpine
 Boron isotopes
 Wechsel area
 Styria

Contents

| | |
|--|-----|
| Zusammenfassung | 325 |
| Abstract | 326 |
| Introduction | 326 |
| Geology | 326 |
| Tourmalinites | 328 |
| Field Observations and Macroscopic Description | 328 |
| Microscopic Description | 329 |
| “Host Rocks” | 332 |
| Geochemistry | 332 |
| General Remarks | 332 |
| Bulk Chemistry | 332 |
| Trace Element Geochemistry | 333 |
| Rare Earth Element Spectra | 333 |
| Boron Isotopic Composition | 333 |
| Microprobe Analyses | 334 |
| Tourmalines | 334 |
| Garnets | 334 |
| Discussion | 336 |
| Conclusions | 338 |
| Appendix | 339 |
| Analytical Methods | 339 |
| Acknowledgements | 340 |
| References | 340 |

Zur Geochemie von Turmaliniten innerhalb der Hüllgesteine des Grobgnesskomplexes

Zusammenfassung

Tourmalinite stellen kleinräumige, jedoch charakteristische lithologische Elemente innerhalb des pre-mesozoischen, kristallinen „Grobgness-Komplexes“, der sich überwiegend aus Phylloniten und dem namengebenden Grobgness zusammensetzt, dar. Die Tourmalinite treten in Form konkordanter, linsenförmiger Körper von wenigen Metern streichender Länge sowie Mächtigkeiten im dm-Bereich ($\leq 0,5$ m) innerhalb der phyllonitischen Gesteine auf. Die Entfernung zwischen den am weitesten auseinander liegenden Fundpunkten beträgt rund 50 km. Die Tourmalinite stellen überwiegend massige, meist schwarze und sehr feinkörnige Gesteine dar. Turmalin (60–80 Vol.-%), Quarz und – stark zurücktretend Muskovit ($\ll 5$ Vol.-%) – sind die einzigen mit dem freien Auge erkennbaren Minerale. Im Dünnschliff sind darüber hinaus Chlorit, Apatit, Klinozoisit, Zirkon und Granat erkennbar. Letzterer enthält zahlreiche kleine Turmalineinschlüsse. Feldspäte fehlen. Die Tourmaline zeigen, unabhängig von ihrer Korngröße, einen einheitlichen Zonarbau mit grünlich-bläulichen Kernbereichen und dunkelbraunen Rändern und entsprechen ihrer chemischen Zusammensetzung nach einem Mg-reichen Schörl. Der Hauptelementchemismus der Tourmalinite wird durch das wechselnde Verhältnis von Turmalin und Quarz kontrolliert, was sich in Bor-Konzentrationen

1 Richard Göd, Friedrich Koller: University of Vienna, Department of Lithospheric Research, Althanstraße 14, 1090 Vienna, Austria. richard.god@univie.ac.at, friedrich.koller@univie.ac.at
 2 Gerhard Heiss: Austrian Institute of Technology, 2444 Seibersdorf, Austria. gerhard.heiss@ait.ac.at

zwischen 2,9 and 8,9 Gew.-% B_2O_3 niederschlägt. Turmalinite und Phyllonite weisen einen äußerst ähnlichen Chemismus auf, der sich nur im hohen Bor- und im niedrigeren Kaliumgehalt der Turmalinite unterscheidet. Der Spurenelementchemismus der Turmalinite ist durch die folgenden Konzentrationen ausgewählter Spurenelemente charakterisiert (arithm. Mitt./Max., ppm; n = 11): Lithium 15/20; Be 4/11, F 790/1280; Sn 13/20 and W 11/30. Die Turmalinite sind frei von jeder Erz- oder Sulfidmineralisation. Die $\delta^{11}B$ -Verhältnisse von ≈ -11 ‰ (5 Analysen; zwei Werte ≈ -9 ‰) entsprechen exakt dem Durchschnittswert der kontinentalen Kruste (Chaussidon & Albarede, 1992). Dieses Ergebnis schließt eine Herkunft des Bors aus marinen Evaporiten für die Turmalinitbildung aus (Barth, 1993; Jiang & Palmer, 1998), erlaubt aber nicht, zwischen einer Herkunft des Bors aus Sedimenten oder einem granitischen Magma zu unterscheiden. Die nahezu identische chemische Zusammensetzung der Turmalinite und Phyllonite spricht für eine Entstehung der Turmalinite durch In-situ-Metasomatose von Sedimenten durch B-reiche hydrothermale Lösungen. Da auch B-reiche Sedimente nicht ausreichend genug Bor enthalten, um Turmalinite im Sinne der Definition zu bilden (z.B. Pesquera et al., 2005), ist eine externe Bor-Zufuhr anzunehmen. Eine zunächst nahe liegende Herkunft des Bors aus dem Grobgneis respektive dessen ursprünglichem Magma erscheint jedoch unwahrscheinlich. Zum einen wegen des Ungleichgewichtes zwischen dem riesigen Volumen des Grobgneises einerseits und der verglichen damit verschwindend kleinen Ausdehnung der Turmalinitkörper und zum anderen wegen des Fehlens jeder Anreicherung von „granitophilen“ Spurenelementen in den Turmaliniten, wie sie im Falle einer Herleitung des Bors aus dem Ausgangsmagma des Grobgneises zu erwarten wären. Daraus folgt, dass die Bildung der beschriebenen Turmalinite zeitlich vor die Intrusion des Ausgangsmagmas des Grobgneises zu stellen ist. Über die Herkunft des Bors kann keine weitergehende Aussage getroffen werden. Die Turmalinite und ihre umgebenden Gesteine sind von zwei metamorphen Überprägungen erfasst worden, die aufgrund regionaler Beobachtungen als permisch respektive spät-kretazisch interpretiert werden (Schuster et al., 2001, 2008). Dies wird durch ein zweiphasiges Wachstum der in den Phylloniten auftretenden Granate unterstrichen. Der ältere Granatkern wird der Permischen Metamorphose zugeordnet, der Rand der spät-Kretazischen. Die Granate innerhalb der Turmalinite hingegen zeigen einphasiges Wachstum, das mit der jüngeren Metamorphose – also mit dem jüngeren Granat aus den Phylloniten – zu korrelieren ist. Die Beobachtung von Turmalineinschlüssen in den Granaten aus den Turmaliniten belegt, dass die Turmalinitbildung älter als die jüngere Granatbildung ist, also voralpidisch. Zusammenfassend lässt sich festhalten, dass die Turmalinite prä-alpin und gleichzeitig älter als das Ausgangsmagma des Grobgneises sind.

Abstract

The tourmalinites investigated are minor but regionally spread lithological elements within the “Grobgneiss Complex”, a tectonic unit predominantly composed of orthogneisses and phyllonites which is part of the pre-Mesozoic crystalline basement of the Eastern Alps. The tourmalinites form small, concordant lenses within the phyllonites with a few meters of lateral extension and thicknesses barely exceeding 0.5 m. The maximum distance between their westernmost and easternmost known occurrences is roughly 50 km. The tourmalinites are mainly fine grained, more/less massive, dark-black rocks. Tourmaline and quartz are the only minerals of significance with tourmaline contents varying between 60 and 80 vol.%. Minor muscovite (<<5 vol.%) may occur locally. Chlorite, apatite, clinozoisite, garnet and zircon are accessory minerals. Garnets display numerous tiny tourmaline inclusions. Feldspars are absent. The tourmalines are zoned with greenish to bluish cores and dark brown rims, their composition corresponds to Mg-rich schorls. Zonation and compositions are uniform regardless of different grain sizes suggesting one tourmaline generation. The bulk chemistry of the tourmalinites is controlled by the mutual relation of tourmaline and quartz as emphasized by B_2O_3 contents varying between 2.9 and 8.9 wt.% and resembles, disregarding the elements boron and potassium, the composition of the hosting phyllonites. The simple trace element pattern of the tourmalinites is inter alia emphasized by the following element concentrations (av./max., ppm, n = 11): Li 15/20; Be 4/11, F 790/1280, Sn 13/20 and W 11/30. The tourmalinites are barren with respect to any kind of mineralization. Their $\delta^{11}B$ values of ≈ -11 ‰ (5 analyses; two values ≈ -9 ‰) match the crustal average (Chaussidon & Albarede, 1992) fairly well. These data preclude marine evaporites as boron sources for the tourmalinites (Barth, 1993; Jiang & Palmer, 1998) but do not allow discrimination between sediments or granites as potential boron sources.

The bulk chemistry of the tourmalinites suggests tourmalinite formation by in situ metasomatism of the hosting meta-sediments (= phyllonites). As even high boron contents in sediments are insufficient to give rise to tourmalinite formation (e.g. Pesquera et al., 2005), an external boron source is necessary. However, the magma parental to the grobgneiss does not seem to be a likely source of boron for the formation of tourmalinites. Firstly due to the imbalance between the huge masses of the precursor magmas of the grobgneiss and the comparable tiny extensions of single tourmalinite bodies and, secondly, due to the trace element chemistry of the tourmalinites not showing any geochemical specification expected to be associated with granite-derived boron-rich fluids. Therefore, tourmalinite formation must have taken place prior to the intrusion of the granitic magma parental to the grobgneiss. Therefore, the origin of boron necessary to form the tourmalinites remains unknown.

The tourmalinites and their host rocks experienced a twofold metamorphic event interpreted as of Permian and of late Cretaceous (= eo-alpine) age respectively (Schuster et al., 2001, 2008). Zoned garnets within phyllonites reflect clearly two garnet generations whereas tourmalinite hosted garnets display a continuous growth which corresponds to the younger garnet generation in the phyllonites. In conclusion, the tourmalinites are therefore pre-Alpine and also older than the magma parental to the grobgneiss.

Introduction

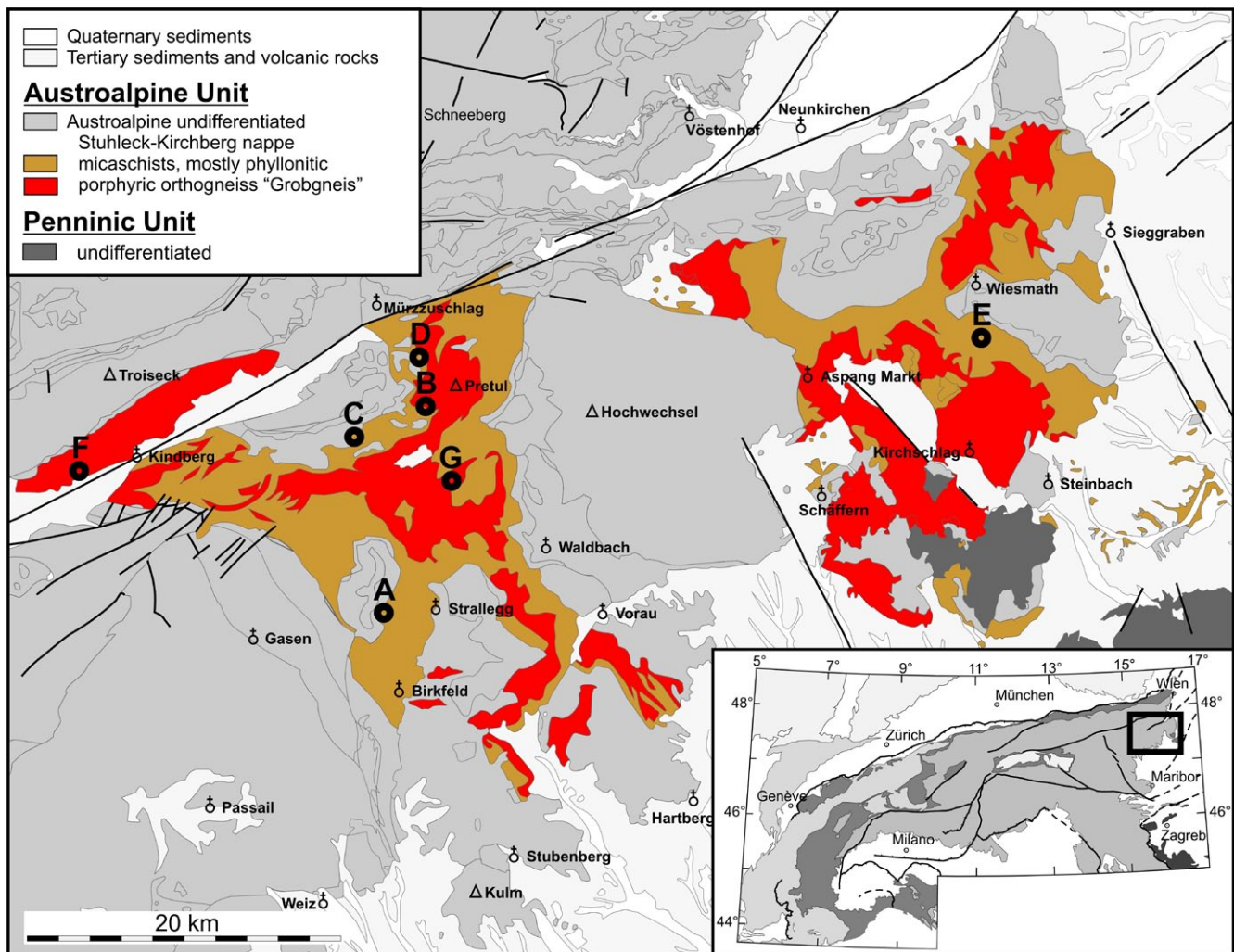
Tourmalinites are by definition stratabound rocks containing ≥ 20 vol.% tourmaline (Slack, 1982; Bates & Jackson, 1987). They are in many cases closely associated with stratabound mineral deposits including e.g. base metals, gold and tungsten and have been found in rocks of Archean to Permian age. Though they are not necessarily mineralized themselves, they are potentially useful as exploration guides (Slack, 1996). Occasionally, the term “tourmalinite” has previously been used for tourmaline-rich rocks irrespective of their geometry. However, in this paper the term is restricted to stratabound tourmalinites only. Tourmalinites in the Alpine Realm related to metavolcanoclastic/metapelitic sequences have been described by Raith (1988), Benvenuti et al. (1989), Zhang et al. (1994) and De Capitani et al. (1999). However, a stratiform arsenopyrite mineralization within the so-called “Grobgneiss Complex”, some 100 km S of Vienna, was found to be spatially associated with tourmalinites (Göd & Heiss, 2007)

and triggered the following study. A first report on the tourmalinites has been published by Göd & Heiss (2009).

The main goal of this paper is the classification of the tourmalinites with emphasis on their petrography, geochemistry and origin.

Geology

Tourmalinites are characteristic but minor lithological elements within a tectonic unit called “Grobgneiss Complex” at the eastern escarpments of the Alps, some 100 km S of Vienna (Text-Fig. 1). The “Grobgneiss Complex” itself is part of the pre-Mesozoic Austroalpine crystalline basement. Phyllonites within this complex enriched in tourmaline were mentioned by Wieseneder (1961), Moreau (1981) and Rockenschaub (1991) but have never been referred to in detail. The regional geology has been extensively compiled by Flügel & Neubauer (1984), Neubauer et al. (1992), Neubauer & Frisch (1993) and Schuster et al. (2001, 2008) (with additional literature herein). Based on



Text-Fig. 1. Simplified geological map of the area investigated in the Eastern Alps. Courtesy R. Schuster, Geological Survey of Austria; the extension of the Stuhleck-Kirchberg nappe is drawn according to Froitsheim et al. (2008); for details of sample locations see Tab. 1.

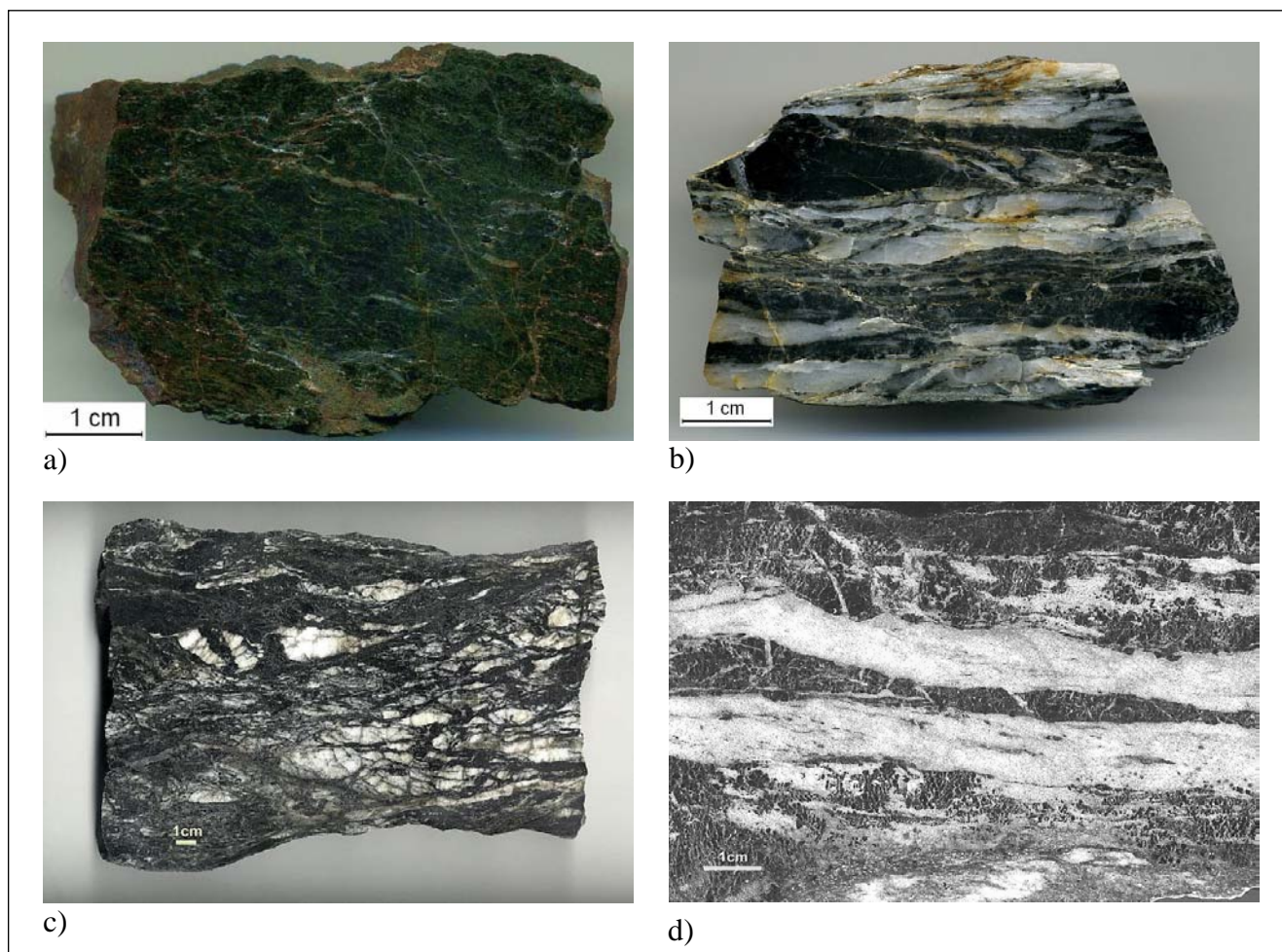
| Sample localities | | ÖK-Sheet | Coordinates (BMN) | Samples |
|-------------------|---|----------|---------------------|--|
| Grablerkogel | A | 135 | RW 701070 HW 253369 | TU10, TU11, TU13, TU26, TU27, TU28, TU33, HR13, HR28, HR33 |
| Pretul | B | 104 | RW 703655 HW 266459 | TU17 |
| Traubachgraben | C | 104 | RW 698995 HW 265789 | TU16 |
| Hirnriegel | D | 104 | RW 703215 HW 270234 | TU14, TU22 |
| Spratzau | E | 106 | RW 744225 HW 271329 | TU29, TU30, TU31, TU32, HR29, HR31 |
| Hadersdorf | F | 103 | RW 680200 HW 263050 | TU40 |
| Ratten | G | 135 | RW 705400 HW 261450 | TU41 |

Table 1. Details of sample localities as shown in Text-Fig. 1.

these authors, the regional geology may be summarized as follows.

The Grobgneiss Complex is predominantly composed of monotonous phyllitic rocks and porphyric orthogneisses (= "grobgneiss"). Meta-Gabbros, amphibolites and paragneisses are additional but rare lithologic elements. The grobgneiss is characterized by large microcline porphyroblasts (up to 3 cm) and experienced a deformation locally

giving rise to phyllonitic textures (Prochaska et al., 1992; Huber, 1994). It is interpreted as a laccolitic body (Flügel & Neubauer, 1984) forming sheet-like bodies with concordant contacts (Neubauer et al., 1992). In terms of its chemistry it has been classified as S-type batholith (Schermaier et al., 1997). Numerous Rb-Sr age determinations of the grobgneiss yield Permian ages around 270 Ma (Schuster et al., 2004).



Text-Fig. 2.
Hand specimens of various types of tourmalinites.
a) black, massive and fine grained type;
b, c) schistose, heavily mylonitized type, locally displaying "quartz-augen" (c);
d) banded tourmalinite.

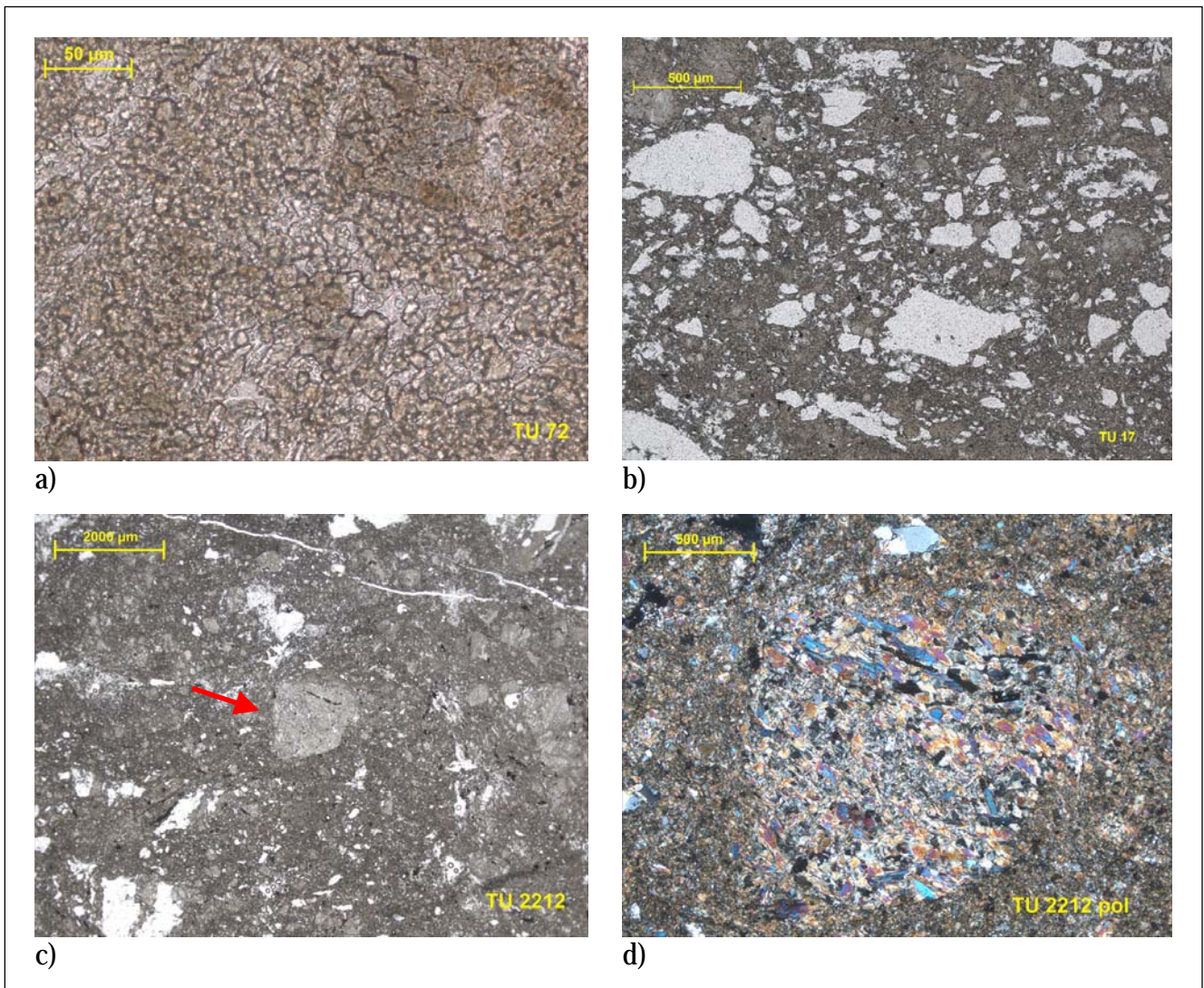
The phyllonitic rocks are fine grained, silvery, greyish to greenish, monotonous and homogeneous rocks composed of mutually varying amounts of quartz, muscovite and chlorite. Due to regionally different grades of metamorphism, chloritized garnet, pseudomorphs after staurolite, biotite, plagioclase, K-feldspar and chloritoid may locally be present. The polyphase evolution of these rocks is emphasized by two separate parageneses: an older one, characterized by Bt (biotite) + Ms (muscovite) + Qtz (quartz) + Grt1 (garnet) + St (staurolite) developed at amphibolite facies conditions and a second, younger one, characterized by the paragenesis Ms + Chl (chlorite) + Qtz + Ab (albite) + Cld (chloritoid) + (Bt) + (Grt2) caused by an upper greenschist to epidote-amphibolite facies giving rise to the diaphthoritic nature of the rocks. The phyllitic rocks are therefore per definition phyllonites. Due to their uniform lithology and monotonous petrographic character no stratigraphy could have been installed so far. The phyllonites (i.e. its precursors) have been intruded by the magma parental to the gneiss but it is still unknown whether the intrusion took place before or contemporaneously with the older metamorphic event as mentioned above. However, it has to be emphasized, that – due to the regional nappe tectonic – no intrusive or any other contact phenomena have ever been observed. The older metamorphic

overprint is interpreted as of Permian age, the younger to be of Cretaceous ("eo-alpine") age which has been dated by Rb-Sr and Ar-Ar methods as varying between 70 Ma and 86 Ma (Schuster et al., 2004, 2008).

Tourmalinites

Field Observations and Macroscopic Description

Tourmalinites per definition have a widespread occurrence as shown in Text-Fig. 1 and Tab. 1. The distance between the easternmost and westernmost occurrence known to date is around 50 km. Single tourmalinite occurrences form concordant lenses as emphasized by minor remnants of phyllonitic host rocks still attached to some boulders. Their lateral extension does not exceed some few tens of meters at the maximum and their thicknesses hardly exceed 0.5 m [It has to be mentioned, that a tourmalinite occurrence displaying a length of 7 m and a thickness of 2 m has been described by Moreau (1981, close to the sample locality A in Text-Fig. 1), but could not be rediscovered]. Considering the comparable small extension of single tourmalinite occurrences, additional as yet unknown occurrences are very likely to exist. Due to the total lack of stratigraphy within the phyllonites it still remains an open question if tourmalinites occur in one or more horizons.



Text-Fig. 3.

Photomicrographs from tourmalinite thin sections.

- a) massive tourmalinite (corresponds to Text-Fig. 2a), displaying a fine grained matrix of xenomorphic tourmaline individuals; the size of single grains may fall below 5 μ ; plane polarized light;
- b) tourmalinite breccia: angular quartz clasts in a fine grained tourmaline matrix (sample corresponds to Text-Fig. 2b); plane polarized light;
- c) tourmalinite breccia composed of randomly oriented angular fragments of tourmalinites (see arrow) in a fine grained tourmaline matrix emphasizing two tectonic overprints;
- d) tourmalinite clast, magnified from Text-Fig. 3c; tourmaline individuals in the clast indicate an older weakly preserved foliation; cross polarized light; textures in c and d are interpreted as textures of an authigenic breccia.

Tourmalinites occur in three different varieties (Text-Fig. 2a-d):

Type 1: Massive, black and extremely fine grained rocks lacking almost any visible schistosity; no single mineral grains are recognizable by the naked eye (Text-Fig. 2a);

Type 2: A somewhat coarser variety with quartz “augen” of cm-size, stressing the schistosity and mylonitic texture of the rock (Text-Fig. 2b, c);

Type 3: Banded tourmalinites; this type is the scarcest, displaying more/less sharply separated layers of tourmaline and quartz with a thickness of a few cm each (restricted to area A in Text-Fig. 1; Text-Fig. 2d).

Owing to the mylonitic texture, none of the tourmalinites display any kind of sedimentary features as frequently described from other locations (e.g. Plimer, 1988; Bandyopadhyay et al., 1990; Slack et al., 1993; Steven & Moore, 1995; Pesquera et al., 2005).

Microscopic Description

The mineralogical composition of all the tourmalinites investigated (about 45 thin sections) is rather uniform. Tourmaline content varies between estimated 60 vol.% and >90 vol.%. The size of single tourmaline crystals varies from <5 μ m (Text-Fig. 3a) in the massive, fine grained type but are somewhat coarser (up to 2 mm) close to the contacts with the hosting phyllonites. All of the individuals, regardless their sizes, display the same optical (and chemical, see chapter “Tourmalines”) zonation with greenish to bluish cores and brown rims. Small grains are xenomorphic, “larger” ones subhedral.

For the most part, tourmaline crystals are randomly oriented, unfoliated and only locally aligned subparallel. A characteristic textural feature are irregularly shaped, randomly oriented angular fragments in a fine grained matrix (Text-Fig. 3b, c) giving rise to a pronounced brecciated texture.

a) **Bulk and trace element chemistry of tourmalinites; main elements wt.%; trace elements ppm**

| | TU11 | TU13 | TU14 | TU16 | TU17 | TU22 | TU27 | TU28 | TU29 | TU32 | TU33 |
|--------------------------------|-------|-------|-------|-------|-------|-------|-------|--------|-------|-------|-------|
| SiO ₂ | 55.4 | 57.08 | 72.76 | 60.16 | 70.88 | 58.27 | 54.77 | 54.15 | 34.67 | 54.08 | 59.03 |
| Al ₂ O ₃ | 22.36 | 20.95 | 13.75 | 18.16 | 15.3 | 20.89 | 21.44 | 22.8 | 33.92 | 23.18 | 21.08 |
| B ₂ O ₃ | 5.76 | 5.34 | 2.9 | 6.15 | 3.03 | 4.86 | 5.67 | 4.35 | 8.89 | 5.99 | 5.34 |
| Fe ₂ O ₃ | 8.15 | 8.53 | 4.82 | 7.31 | 3.79 | 7.48 | 8.8 | 9.65 | 12.58 | 8.59 | 7.68 |
| MgO | 3.26 | 3.33 | 1.35 | 2.87 | 1.87 | 2.37 | 3.38 | 3.75 | 4.19 | 3.1 | 2.38 |
| MnO | 0.03 | 0.04 | 0.05 | 0.04 | 0.01 | 0.12 | 0.04 | 0.04 | 0.09 | 0.06 | 0.05 |
| CaO | 0.4 | 0.37 | 0.12 | 0.2 | 0.14 | 0.2 | 0.43 | 0.47 | 0.38 | 0.4 | 0.37 |
| Na ₂ O | 0.96 | 0.95 | 0.72 | 1.02 | 0.79 | 1.16 | 0.96 | 1.04 | 1.36 | 0.91 | 0.92 |
| K ₂ O | 0.15 | 0.11 | 0.94 | 0.88 | 1.36 | 1.11 | 0.2 | 0.04 | 0.08 | 0.1 | 0.32 |
| TiO ₂ | 1.22 | 0.81 | 0.67 | 0.75 | 0.65 | 0.86 | 1.57 | 0.94 | 0.8 | 0.83 | 0.71 |
| P ₂ O ₅ | 0.04 | 0.03 | 0.05 | 0.08 | 0.01 | 0.05 | 0.04 | 0.03 | 0.02 | 0.09 | 0.16 |
| LOI | 2.15 | 2.25 | 1.62 | 2.35 | 2.13 | 2.24 | 2.65 | 2.75 | 2.98 | 2.56 | 1.94 |
| SUM | 99.88 | 99.79 | 99.75 | 99.97 | 99.97 | 99.61 | 99.95 | 100.01 | 99.96 | 99.89 | 99.98 |

| | | | | | | | | | | | |
|----|-----|------|------|------|------|------|-----|-----|-----|------|-----|
| Li | 12 | 15 | 14 | 23 | 8 | 16 | 19 | 14 | 20 | 15 | 11 |
| F | 550 | 670 | 930 | 1280 | 1040 | 1230 | 640 | 600 | 590 | 490 | 710 |
| Cl | --- | 22 | <14 | <14 | 19 | --- | --- | --- | --- | 23 | --- |
| Br | --- | <0.7 | <0.5 | <0.5 | <0.5 | --- | --- | --- | --- | <0.5 | --- |
| I | --- | <0.5 | <0.5 | <0.5 | <0.5 | --- | --- | --- | --- | <0.5 | --- |

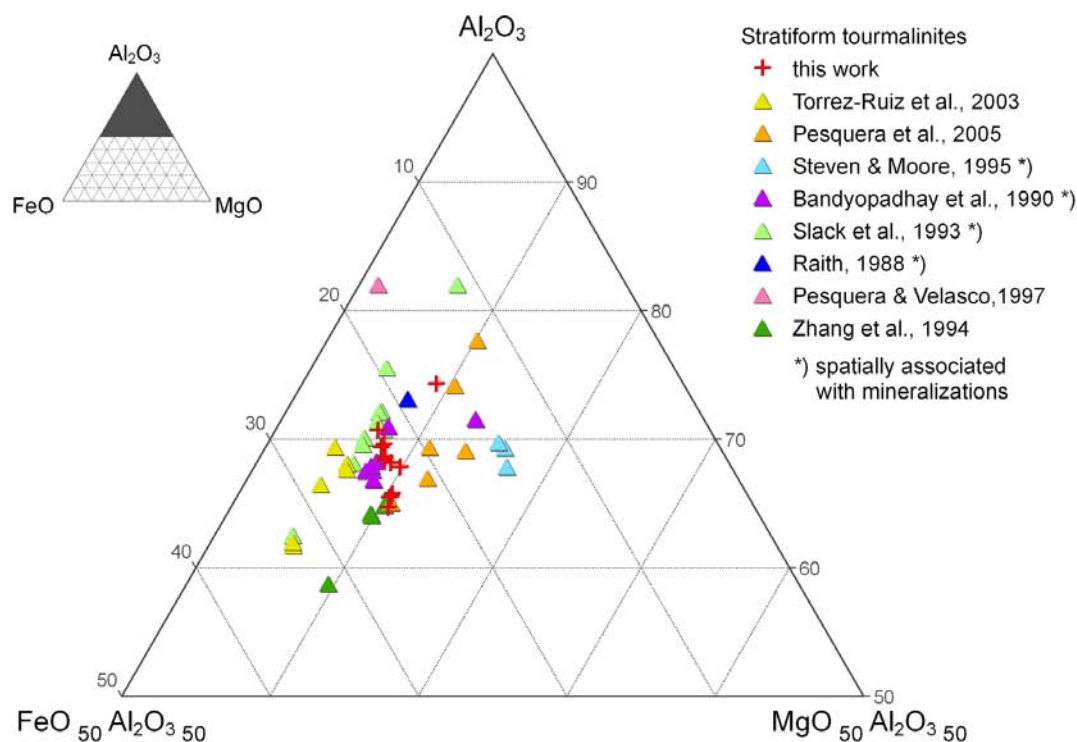
| | | | | | | | | | | | |
|--------|-------|-------|-------|-------|-------|-------|-------|-------|-------|-------|-------|
| Pb | 1 | 2 | 3 | 2 | 3 | 3 | 1 | 2 | 7 | 6 | 2 |
| Zn | 17 | 28 | 2 | 12 | 2 | 1 | 27 | 31 | 22 | 24 | 13 |
| Cu | 20 | 16 | 12 | 1 | 2 | 6 | 34 | 20 | 17 | 26 | 22 |
| Mo | 4 | 3 | 2 | <1 | 1 | 2 | 1 | 3 | 1 | <1 | <1 |
| Ni | 53 | 50 | 9 | 50 | 182 | 14 | 46 | 36 | 40 | 39 | 40 |
| As | 4 | 8 | 87 | 48 | 22 | 29 | 2 | 8 | 45 | 14 | 1 |
| Sb | <0.1 | <0.1 | 0.1 | <1 | 0.1 | 0.2 | 0.1 | <0.1 | <0.1 | <0.1 | <0.1 |
| Se | <0.5 | <0.5 | <0.5 | <0.5 | <0.5 | <0.5 | <0.5 | <0.5 | <0.5 | <0.5 | <0.5 |
| Hg | <0.01 | <0.01 | <0.01 | <0.01 | <0.01 | <0.01 | 0.01 | <0.01 | <0.01 | <0.01 | <0.01 |
| Cd | <0.01 | <0.01 | <0.01 | <0.01 | <0.01 | <0.01 | 0.1 | <0.01 | <0.01 | <0.01 | <0.01 |
| Tl | <0.1 | <0.1 | <0.1 | <0.1 | <0.1 | <0.1 | <0.1 | <0.1 | <0.1 | <0.1 | <0.1 |
| Au ppb | 7 | 5 | 1 | 3 | 1 | 1 | 148 | 46 | 4 | 1 | 1 |
| Ag | <0.01 | <0.01 | <0.01 | <0.01 | <0.01 | <0.01 | <0.01 | <0.01 | <0.01 | <0.01 | <0.01 |
| Bi | 1 | 14 | 1 | 1 | <1 | <1 | 18 | 29 | <1 | <1 | <1 |
| Sn | 18 | 10 | 9 | 11 | 20 | 18 | 16 | 12 | 11 | 7 | 6 |
| W | 7 | 2 | 2 | 4 | 132 | 2 | 7 | 16 | 11 | 24 | 30 |
| U | 1 | 1 | 2 | 2 | 2 | 2 | 2 | 1 | 3 | 2 | 3 |
| Th | 9 | 7 | 10 | 13 | 8 | 15 | 13 | 9 | 9 | 14 | 14 |
| Zr | 184 | 173 | 290 | 136 | 208 | 228 | 243 | 198 | 166 | 166 | 215 |
| Hf | 5 | 5 | 9 | 4 | 6 | 7 | 7 | 6 | 5 | 5 | 6 |
| Ga | 32 | 27 | 18 | 24 | 20 | 27 | 30 | 31 | 49 | 32 | 26 |
| Rb | 8 | 5 | 45 | 44 | 53 | 53 | 10 | 1 | 3 | 4 | 12 |
| Sr | 54 | 51 | 85 | 88 | 50 | 122 | 56 | 56 | 98 | 146 | 100 |
| Cs | <1 | <1 | 2 | 2 | 1 | 2 | <1 | <1 | <1 | <1 | <1 |
| Be | 1 | 1 | 4 | 3 | 5 | 6 | 1 | 1 | 11 | 6 | 2 |
| Ba | 24 | 11 | 111 | 87 | 228 | 108 | 24 | 1 | 9 | 24 | 61 |
| Sc | 8 | 6 | 12 | 16 | 12 | 18 | 12 | 8 | 15 | 19 | 15 |

b) **Statistical summary**

| | Tourmalinites n = 11 | | | | Phyllonites n = 48 | | | | "Host rocks" n = 4 | | |
|--------------------------------|----------------------|-------|-------|--|--------------------|-------|-------|--|--------------------|-------|-------|
| | min. | max. | med. | | min. | max. | med. | | min. | max. | mean |
| SiO ₂ | 34.67 | 72.76 | 56.24 | | 42.69 | 85.96 | 63.01 | | 28.30 | 43.02 | 31.19 |
| Al ₂ O ₃ | 13.75 | 33.92 | 21.26 | | 6.90 | 31.36 | 17.26 | | 30.62 | 35.86 | 33.29 |
| B ₂ O ₃ | 2.90 | 8.89 | 5.51 | | - | - | - | | - | - | - |
| Fe ₂ O ₃ | 3.79 | 12.67 | 8.34 | | 1.89 | 10.64 | 5.69 | | 15.74 | 21.08 | 18.42 |
| MgO | 1.35 | 4.23 | 3.18 | | 0.66 | 5.03 | 2.22 | | 3.76 | 5.55 | 4.56 |
| MnO | 0.01 | 0.12 | 0.05 | | 0.01 | 0.22 | 0.06 | | 0.09 | 0.33 | 0.13 |
| CaO | 0.12 | 0.47 | 0.38 | | 0.01 | 5.77 | 0.41 | | 0.08 | 0.10 | 0.09 |
| Na ₂ O | 0.72 | 1.36 | 0.96 | | 0.06 | 6.10 | 1.49 | | 0.60 | 0.98 | 0.77 |
| K ₂ O | 0.04 | 1.36 | 0.18 | | 0.86 | 5.92 | 3.69 | | 0.97 | 4.38 | 2.67 |
| TiO ₂ | 0.65 | 1.57 | 0.82 | | 0.20 | 1.43 | 0.84 | | 2.38 | 2.67 | 2.48 |
| P ₂ O ₅ | 0.01 | 0.16 | 0.04 | | 0.02 | 0.21 | 0.12 | | 0.03 | 0.05 | 0.04 |

Table 2.

a) Bulk and selected trace element chemistry of tourmalinites; for methods used see appendix; b) Statistical summary of the bulk compositions of tourmalinites, phyllonites and host rocks; data on phyllonites include analysis of Schafflechner (2002), Göd & Heiss (2007) and Bernhard (2006).



Text-Fig. 4a.

Ternary FeO-Al₂O₃-MgO plot showing whole-rock compositions (wt.%) of stratiform tourmalinites from this work and from literature based on a total of 56 analyses. The relevant geological environments are summarized in Tab. 2; geochemical similarities to the data of this work exist to tourmalinites from the Broken Hill district and to tourmalinites from the Sakoli group/central India; bulk chemistries of barren and mineralized tourmalinites do obviously not differ.

| Reference | Host rock | Metam. grade | Age | Mineralization |
|----------------------------|--|---|-------------------------------|----------------|
| Torrez Ruiz et al., 2003 | garnet bearing pelitic schists, mica schists | greenschist facies, retrograde | Permo-Triassic | barren |
| Pesquera et al., 2005 | psammopelitic rocks calc silicate schists | low-medium grade, staurolite facies; | upper to late Proterozoic | mineralized |
| Steven & Moore, 1995 | biotite-muscovite schists | green schist – upper amphibolite facies; | late Proterozoic | mineralized |
| Bandyopadhyay et al., 1990 | pelitic schists; felsic & mafic metavolcanics | green schist facies | early to mid- Proterozoic | mineralized |
| Slack et al., 1993 | psammopelitic to psammitic schists; | amphibolite – granulite facies | early Proterozoic | mineralized |
| Raith, 1988 | metaclastic rocks, calc silicates | upper greenschist to amphibolite facies | lower Palaeozoic | mineralized |
| Pesquera & Velasco, 1997 | carbonaceous metapelites | andalusite-garnet- biotite zone | Palaeozoic (Carboniferous) | barren |
| Zhang et al., 1997 | metaclastic rocks | lower greenschist facies | Permian | barren |

Table 3.

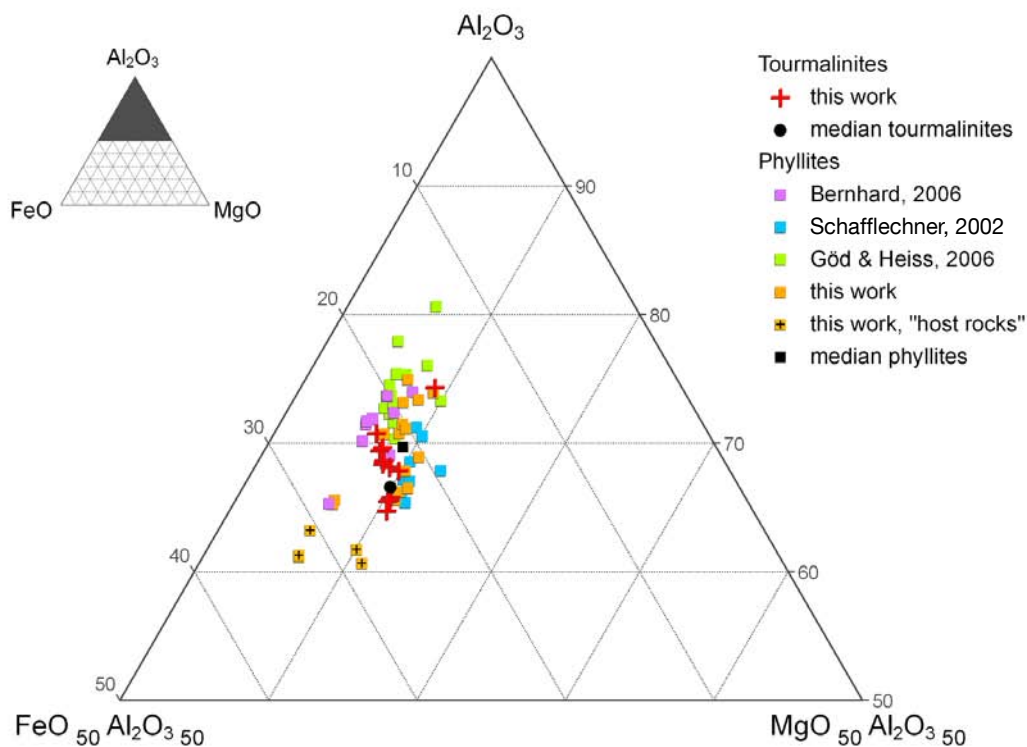
Geological environment of the stratiform tourmalinites as plotted in Text-Fig. 4a, terminology according to the authors as cited.

The fragments display the same mineralogy and grain sizes as the tourmalinites themselves and doubtlessly post-date the lithification of the tourmalinite (Text-Fig. 3c, d). This texture corresponds exactly to what is called an auligenic breccia. Almost identical textures have been described from tourmalinites in the Orobic Alps (Zhang et al., 1994) and in the Proterozoic Kuiseb Formation, Namibia (Steven & Moore, 1995, p 1109).

The secondmost abundant mineral is quartz. Lenses of quartz – from microscopic scale up to cm-size – under-

line the schistosity and the mylonitic texture of some of the specimens (Text-Fig. 2c). All quartz aggregates are totally recrystallized forming subgrains with undulose extinction.

Muscovite and chlorite are minor components, altogether contributing not more than approx. 5 vol.% to the modal composition. Tiny, rounded zircons – giving rise to pleochroitic haloes in tourmalines – apatite, titanite and clinozoisite are accessory minerals. Subhedral garnets, less than 0.5 mm in size, have been observed in two samples only (see also chapter “Garnets”). Garnet individuals



Text-Fig. 4b.

Ternary $FeO-Al_2O_3-MgO$ plot comparing bulk chemistries (wt.%) of tourmalinites (this work) and surrounding phyllonites.

Tourmaline chemistries plot well together with the compositions of the phyllonites (48 analyses). Squares with crosses (symbol) refer to supposedly altered phyllonites at the contact to tourmalinites (= "host rocks" in chapter "Host Rocks").

include numerous inclusions of tourmaline grains indicating the garnets to be younger than the tourmalines. Chloritoid is restricted to contacts between tourmalinites and host rocks (see below). All tourmalinites investigated are free of biotite and feldspars.

"Host Rocks"

Some of the tourmalinite boulders show minor remnants of phyllonitic rocks still "sticking" on them indicating the tourmalinites to be concordant to main schistosity of their host rocks. These may be described as greyish-green, finely laminated phyllonitic rocks containing up to 60 vol.% chloritoid plus muscovite, chlorite, quartz and some minor tourmaline. The chloritoid content decreases with growing distance (cm-range) to the contact. The immediate contact (mm-scale) between tourmalinite and its host rock is also significantly enriched in titanite. The chemistry of these "contact rocks" differs from the composition of the "normal" phyllonites (Tab. 2b; Text-Fig. 4b).

Geochemistry

General Remarks

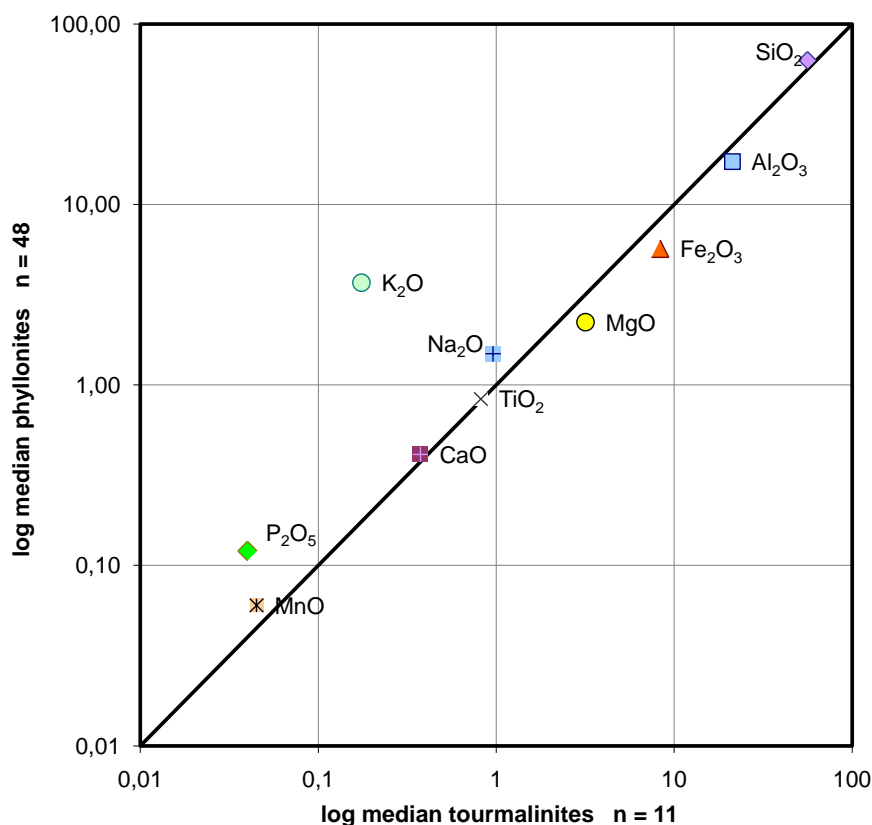
A total of 11 tourmalinites and 20 phyllonites have been analysed for their bulk and trace-element chemistry. Five of the tourmalinites have been additionally analysed for the halogenes chlorine, bromine and iodine. The results are listed in Tab. 2a and b. Seven tourmaline samples have been investigated for their $^{11}B/^{10}B$ isotopic ratio (Tab. 4). The analytical methods used are summarized in the "appendix" at the end of this paper.

Bulk Chemistry

The bulk chemistry displays significantly varying contents of SiO_2 (34.67–72.76 wt.%), Al_2O_3 (13.75–33.92 wt.%), B_2O_3 (2.9–8.89 wt.%), Fe_2O_3 (3.79–12.67 wt.%) and MgO (1.35–4.23 wt.%) (Tab. 2a). It is controlled by the simple mineralogical composition as described and therefore by the mutual relation of tourmaline and quartz. The very low content of CaO (0.12–0.47 wt.%) and K_2O (0.04–1.36 wt.%) has to be emphasized in particular.

The ternary plot $FeO - Al_2O_3 - MgO$ combines analytical results from this work and data from stratiform tourmalinites from literature (Text-Fig. 4a; the plot is based on a total of 60 analyses). With one exception, all tourmalinite samples of this work cluster fairly well and correspond with many of the data as cited. The closest similarity – in terms of bulk composition – exists to Proterozoic tourmalinites from the Broken Hill area/Australia (Slack et al., 1993) and from the "Sakoli Group" in central India (Bandyopadhyay et al., 1990).

Bulk chemistries of tourmalinites from this work and phyllonites from the Grobgness Complex are plotted together in Text-Fig. 4b. It should be stressed, that these phyllonites do not host the tourmalinites as such, but have been sampled across the Grobgness Complex. However, the phyllonites, as cited, are assumed to be fairly well representative for the phyllonites of that unit (the plot is based on a total of 48 analyses). The plot emphasizes the close similarity of the bulk chemistries of tourmalinites and phyllonites respectively. The samples separated from the main cluster plotting closest to the $FeO-Al_2O_3$ corner of the ternary are the "host rocks" as described in chapter "Host Rocks".



Text-Fig. 5. Comparison of median concentrations (bulk chemistries, log C) of tourmalinites and phyllonites displaying the striking similarities of their bulk chemistries. Exceptions are potassium and, to a lesser extent, sodium.

The similarity of the bulk chemistries of tourmalinites and phyllonites is additionally stressed by plotting their main element concentrations (Text-Fig. 5). Concentrations of silica and immobile elements in tourmalinites and phyllonites are identical, the concentrations of iron and magnesium differ just slightly. However, the tourmalinites are significantly depleted in potassium and to a lesser degree in sodium.

Trace Element Geochemistry

The tourmalinite samples have been analysed for a total of 45 trace elements. The simple trace element pattern mirrors the comparably simple bulk geochemistry as discussed. None of the element concentrations exceeds the relevant geochemical background values for crustal rocks significantly. However, concentrations of some selected elements considered to be of possible relevance for the genetic interpretation of tourmalinites are listed in Tab. 2a. Lithium and beryllium concentrations (med./max.) of 15/22 ppm and 4/11 ppm match the crustal average whereas tin and tungsten concentrations of 11/20 and 9/30 ppm respectively surpass insignificantly the average crustal abundances of 2.5 ppm and 1.4 ppm respectively (data according to Wedepohl, 1995). The same holds for fluorine (790/1280 ppm) compared to a crustal average of 600 ppm. A slight enrichment of arsenic concentrations of 14/87 ppm of the tourmalinites compared to 2 ppm for the continental crust (Wedepohl, 1995) is in accordance with regionally elevated arsenic contents of the phyllonites within the Grobgneiss Complex (Göd & Heiss, 2007).

Taking into consideration a possible derivation of the tourmalinites from marine evaporites assumed to be enriched in iodine, bromine and chlorine and considering the possibility of these elements to be trapped in fluid inclusions,

five samples have been analysed for these elements yielding the following results: iodine and bromine <0.5 ppm and chlorine contents of \approx 20 ppm for three of the analysed samples – far below the average abundances in shales and schists of around 1–6 ppm for iodine and bromine respectively and for chlorine of 200 ppm as summarized by Reimann & Caritat (1998).

Rare Earth Element Spectra

The rare earth element patterns of phyllonites, host rocks and tourmalinites are very similar (Text-Fig. 6) indicating the tourmalinites to have the lowest absolute contents of Σ REE: tourmalinites 131 ppm; host rocks: 193 ppm; phyllonites: 418 ppm and, for comparison, “average shales” in the sense of Turekian & Wedepohl (1961): 207 ppm.

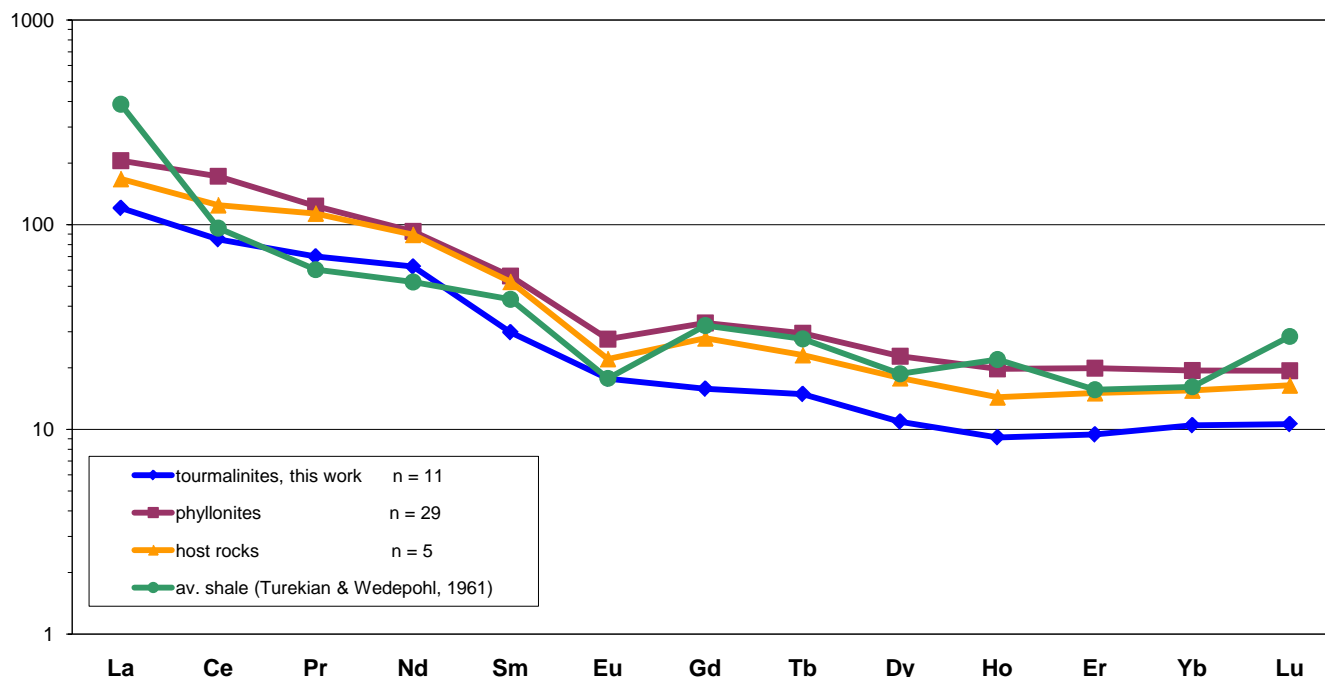
Boron Isotopic Composition

Due to the large relative mass difference between $\delta^{10}\text{B}$ (relative abundance: 20 %) and $\delta^{11}\text{B}$ (relative abundance: 80 %), geological environments display large variations in their $^{11}\text{B}/^{10}\text{B}$ ratios ranging between -30 ‰ and approx. +60 ‰ as summarized by Barth (1993) and Palmer & Swihart (1996) (Text-Fig. 7). The average $\delta^{11}\text{B}$ value of the continental crust is “bracketed” between -8 ‰ and -13 ‰ (\approx 10 ‰; Chaussidon & Albarede, 1992).

Five samples of tourmaline concentrates from tourmalinites (TU11, TU13, TU14, TU17 and TU32 respectively, Text-Fig. 1) and two samples of tourmalines from veins within the grobgneiss (TU40 and TU41) have been analysed for their $^{11}\text{B}/^{10}\text{B}$ ratios. The results are given in Tab. 4.

Disregarding TU17 and TU41, boron isotope compositions of tourmalines from tourmalinites and one of the grobgneiss-hosted tourmaline veinlets (TU40) are extremely

Chondrite normalized whole-rock REE patterns



Text-Fig. 6. Chondrite normalized (based on McDonough & Sun, 1995) plot of REE abundances in rock types investigated, underlining the almost identical patterns of the rock types dealt with.

similar, displaying an averaging $\delta^{11}\text{B}$ value of -11.2% (Text-Fig. 7) – in full agreement with the average value of the continental crust. However, boron isotope compositions of TU17 and TU41 differ slightly displaying $\delta^{11}\text{B}$ values of -9.15% and -9.34% respectively and occur in different geological environments: sample TU17 represents an extremely mylonitized, phyllonite hosted tourmalinite (Text-Fig. 2b) of some 20 cm thickness, whereas sample TU41 has been taken from a tourmaline bearing veinlet of some 10 cm thickness within the gneiss. The sample localities are about 25 km apart.

Microprobe Analyses

Tourmalines

A total of 31 tourmaline individuals from sample sites A, D and E (Text-Fig. 1) have been analysed (methods used see

| Sample | Host rock | $\delta^{11}\text{B}$ |
|--------|--------------|-----------------------|
| TU11 | Tourmalinite | -11.37 ± 0.45 |
| TU13 | Tourmalinite | -11.17 ± 0.37 |
| TU14 | Tourmalinite | -10.61 ± 0.40 |
| TU17 | Tourmalinite | -9.15 ± 0.35 |
| TU32 | Tourmalinite | -11.52 ± 0.47 |
| TU40 | Gneiss | -11.31 ± 0.37 |
| TU41 | Gneiss | -9.43 ± 0.32 |

Table 4. Boron-isotope compositions of tourmaline concentrates. Analyst: S. Tonarini, Geosciences and Georesources Institute of Italian National Research Council, Pisa; IGG-CNR; for sample localities see Text-Fig. 1 and Tab. 1.

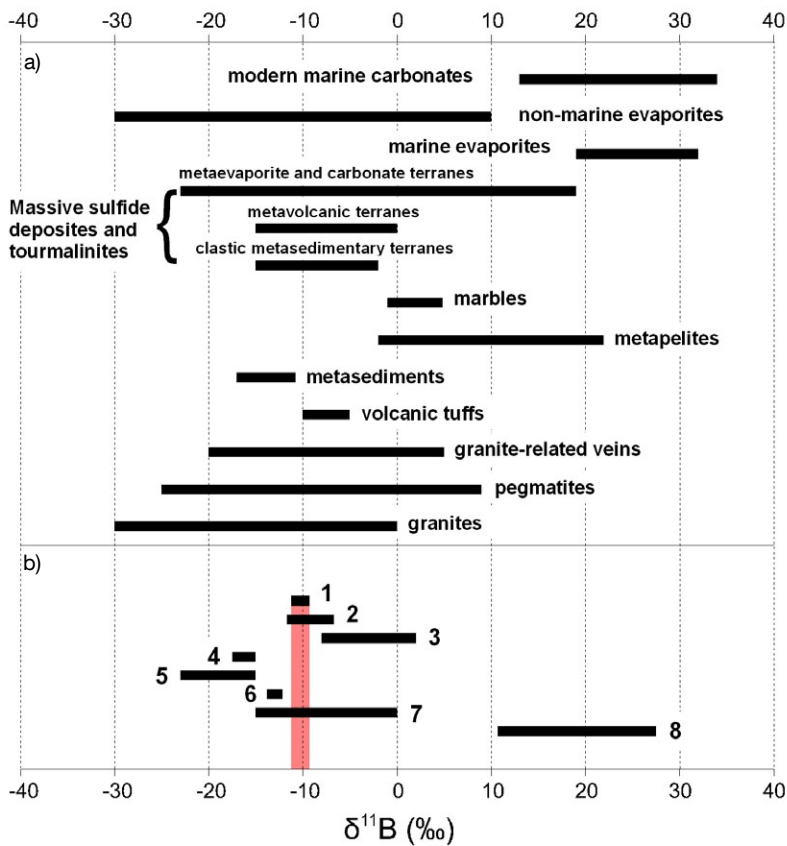
appendix), the results are plotted – together with tourmaline analyses from stratabound tourmalinites from literature – in the ternary diagram Al – Fe – Mg (Henry & Guidotti, 1985; Text-Fig. 8). This diagram classifies and discriminates tourmaline compositions according to their petrographic background. Tourmaline compositions of this work cluster into the field “2” = “tourmalines from Li-poor granitoids and their associated pegmatites and aplites” and overlapping slightly field “4” = “tourmalines from metapelites and metapsammities coexisting with an Al-saturating phase”. Tourmaline chemistries most similar to the ones presented are found in the “Sakoli” group/Central India (Bandyopadhyay et al., 1990) as already referred to in context with the bulk chemistry of the tourmalinites.

The tourmalines display a significant variety of zonation patterns ranging from weak to irregular patchy zoning to fine-scale oscillatory zoning. Tourmaline cores display FeO contents of approximately 7 wt.% and MgO contents of approximately 6 wt.%, whereas rims are higher in FeO, around 12 wt.%, and poor in MgO, approximately 2.5 wt.%.

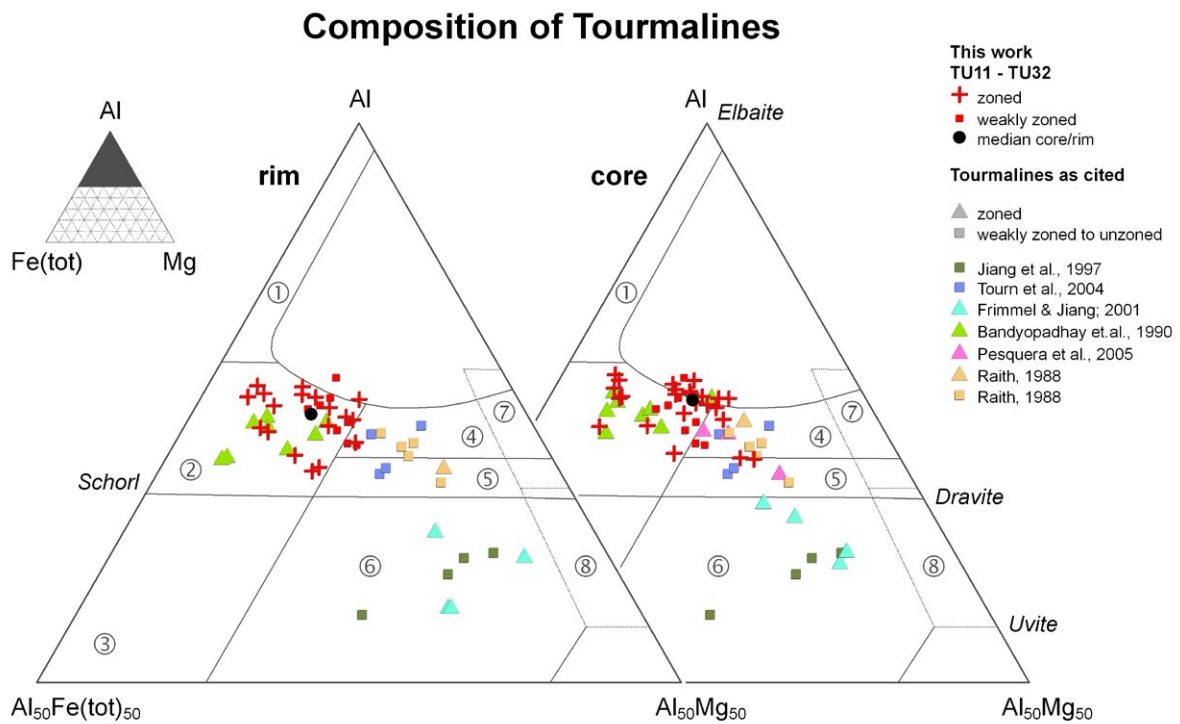
Occasionally, contrary zonations – MgO-poor and FeO-rich cores – have been observed as well, however, a detailed investigation of this observation is beyond the scope of this paper. Chemistry and zonation of tourmaline individuals are not related to their grain size stressing the existence of just one tourmaline generation.

Garnets

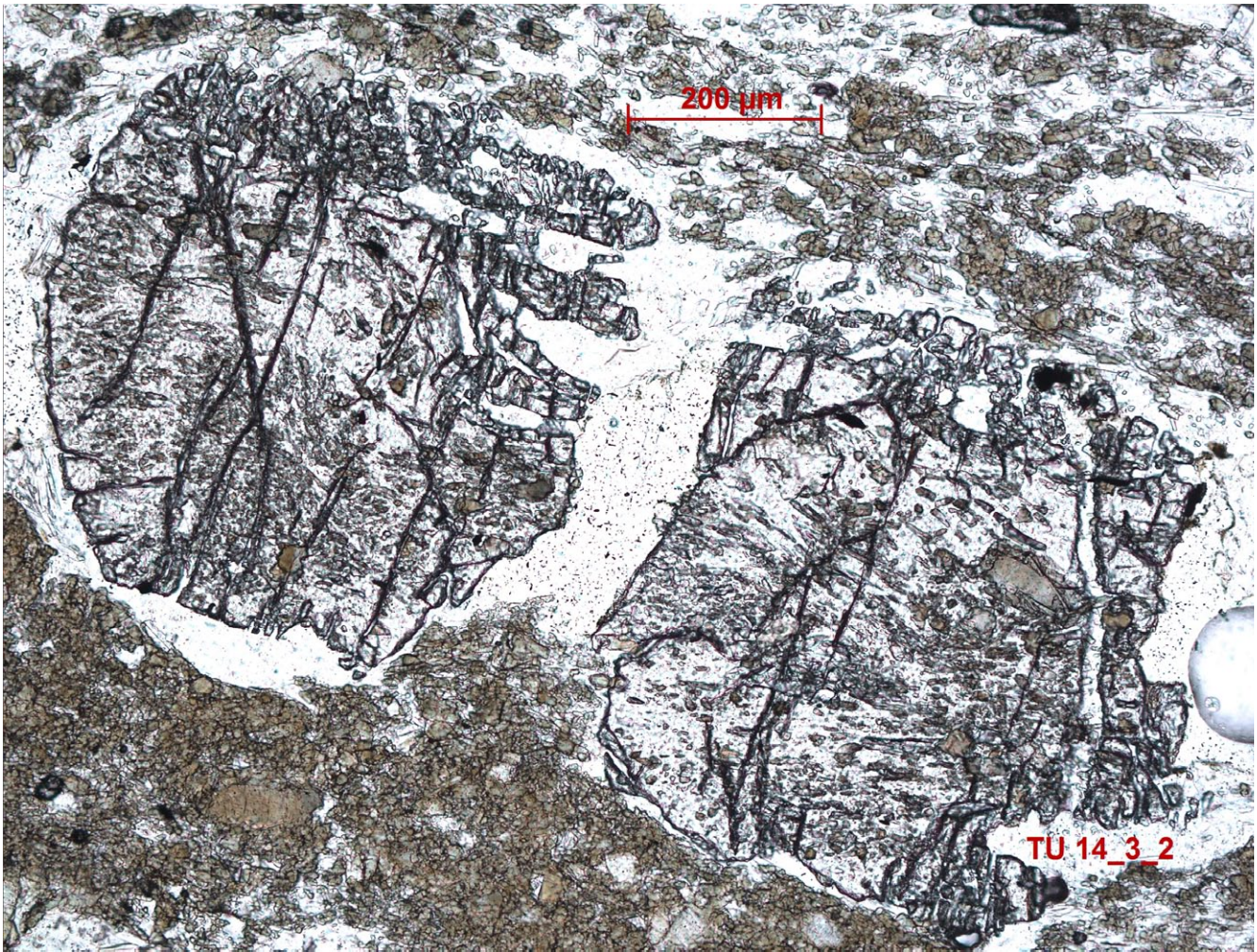
Garnets are minor, subordinated components in tourmalinites and phyllonites alike. Tourmalinite hosted individuals are subhedral, sometimes aligned parallel to the



Text-Fig. 7.
 a) Boron-isotope variations in selected lithologies and geological environments summarized and simplified after Barth (1993), Palmer & Swihart (1996) and Jiang & Palmer (1998).
 b) boron-isotope variations of stratiform tourmalinites:
 1) this work;
 2) Trumbull et al. (2008)
 3) Pesquera et al. (2005)
 4) Jiang (2001);
 5) Jiang et al. (1999);
 6) Bandyopadhyay et al. (1990);
 7) Chaussidon & Albarede (1992);
 8) Frimmel & Jiang (2001);
 these data point to tourmalinites of evaporitic origin and are clearly separated from data of tourmalinites of any other origin.



Text-Fig. 8.
 Ternary Al-Fe-Mg plot of tourmaline compositions from stratiform tourmalinites; data fields after Henry & Guidotti (1985);
 1: Li-rich granitoids and their associated pegmatites and aplites;
 2: Li-poor granitoids and their associated pegmatites and aplites;
 3: Fe³⁺-rich quartz-tourmaline rocks (hydrothermally altered granites);
 4: metapelites and metapsammities coexisting with an Al-saturating phase;
 5: metapelites and metapsammities not coexisting with an Al-saturating phase;
 6: Fe³⁺-rich quartz-tourmaline rocks, calc-silicate rocks and metapelites;
 7: low Ca meta-ultramafics;
 8: metacarbonates and metapyroxenites.



Text-Fig. 9. Subhedral garnet individuals inbedded in a fine grained tourmaline-quartz matrix, plane polarized light; note the tourmaline inclusions proving the garnets to be younger than the tourmalines.

schistosity and display small grain sizes generally below 0.5 mm. All of them include numerous, tiny tourmaline inclusions as mentioned (Text-Fig. 9) emphasizing the age relation between these minerals. Due to the diaphthoritic overprint, the phyllonite hosted garnets are generally chloritized and frequently display clusters of grains forming some sort of “garnet plaster”. Analytical data of single grains in the “garnet plaster” may therefore cause “erratic” results leading to “inconsistence” zonal element distributions i.e. contradicting zonalities.

As shown in the ternary diagram almandine – grossular + spessartine – pyrope (Text-Fig. 10) tourmalinite and phyllonite hosted garnets plot in distinct, separate clusters and may be described as follows:

- Tourmalinite hosted garnets are generally higher in spessartine and grossular and display a narrow range in composition (Text-Fig. 10). The uniform shape of their zonality (Text-Fig. 11c) points clearly to a one-phase growth. Garnet cores are low in pyrope and almandine and high in spessartine whereas rims are higher in almandine and pyrope and lower in spessartine.
- Phyllonite hosted garnets, on the contrary, display a wide range in their chemical composition caused by their varying almandine content (Text-Fig. 10). Zonal

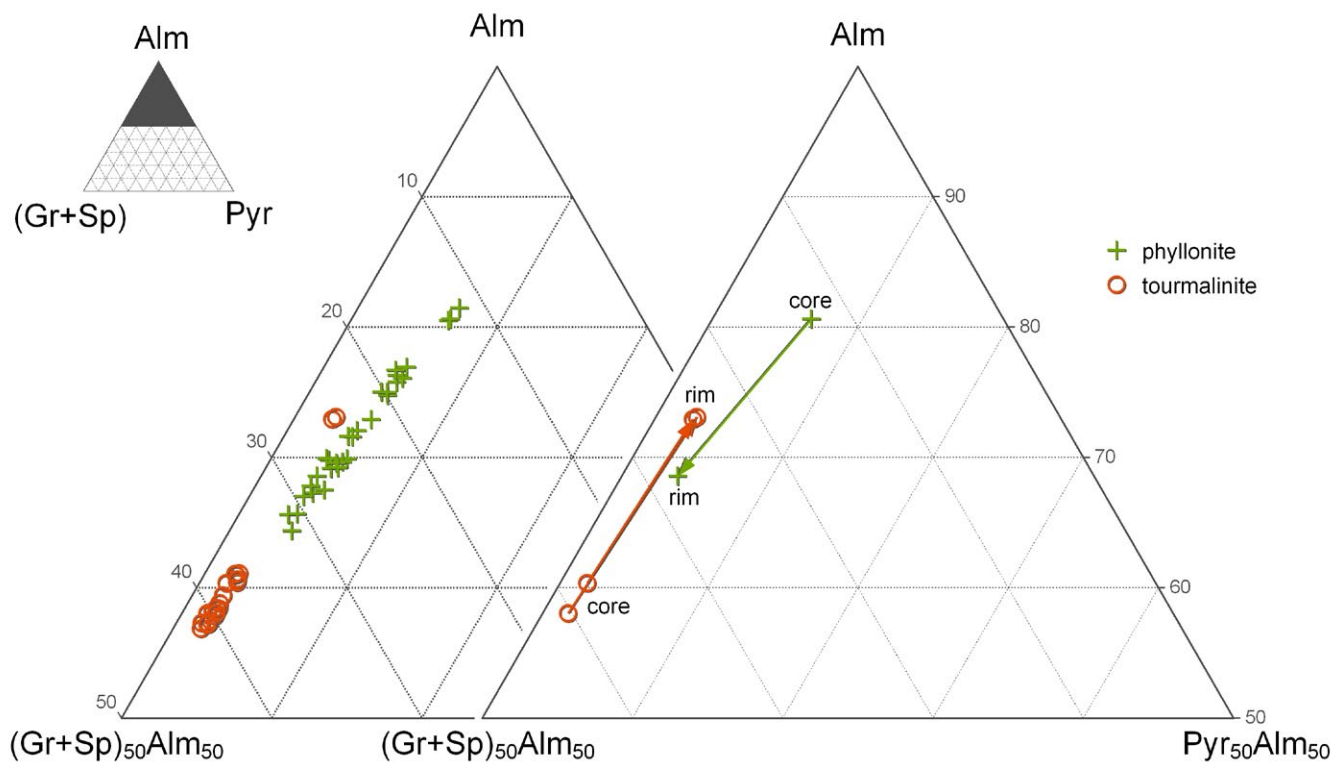
distribution of elements (Text-Fig. 11d) points clearly to a two-phase growth with cores rich in almandine and pyrope and poor in spessartine and grossular (in contradiction to the tourmaline hosted garnets!). The rims, however, display a zonal element distribution themselves indicating an outwards increase in almandine and pyrope content (Text-Fig. 11d, see in particular the right half of the plot) which corresponds perfectly to the zonality as shown by the tourmaline hosted garnets in Text-Fig. 11c).

Almandine-rich cores of phyllonite hosted garnets are therefore interpreted as relics of an older garnet generation whereas their rims and the tourmalinite hosted garnets are interpreted as contemporaneously grown, belonging to a young garnet generation. The variance in almandine content as shown in Text-Fig. 10 mirrors garnet compositions between these two generations caused by the analyses of “subgrains” of the “garnet plaster” as mentioned.

Discussion

The origin of tourmalinites has been a matter of permanent controversy and has been extensively summarized by numerous authors (e.g. by Slack, 1996; Torrez-Ruiz et al., 2003). According to these summaries, the following

Composition of Garnets



Text-Fig. 10.

Alm-(Gr+Sp)-Py plot of garnets from tourmalinites and phyllonites (left side) and corresponding contrary zonal compositions (right side); note the comparable homogeneous compositions of the tourmalinite hosted garnets compared to the wide range of garnet composition in the phyllonites. This wide range mirrors any compositions between cores and rims in phyllonite hosted garnets.

processes may give rise to the formation of tourmalinites: a) precipitation from exhalative fluids; b) premetamorphic hydrothermal replacement of aluminous sediments, c) diagenesis and metamorphism of B-rich sediments or evaporites, d) metasomatism by B-rich fluids of magmatic or metamorphic affiliation or, at least, a combination of these models.

The bulk chemistry of the tourmalinites as analysed is in good agreement with numerous data from literature (Text-Fig. 4a). Geochemical affinities exist with tourmalinites from the Broken Hill District, Australia (Slack et al., 1993), with tourmalinites of the Sakoli Group, Nagpur district, central India (Bandyopadhyay et al., 1990), with tourmalinites in the Austroalpine Crystalline Complex, Austria (Raith, 1988), all of them spatially associated with mineralizations. However, bulk chemistries of tourmalinites are controlled by their surrounding lithologies (Text-Fig. 4a and Tab. 3) whereas barren or mineralized tourmalinites do obviously not differ systematically in their composition.

The close geochemical similarity between tourmalinites and the hosting phyllonites is shown in Text-Fig. 4b by overlapping clusters of analytical data in the ternary system $\text{Al}_2\text{O}_3 - \text{FeO} - \text{MgO}$. This relationship is additionally emphasized by plotting the average major element distributions of tourmalinites and phyllonites respectively (Text-Fig. 5). Disregarding the boron, the potassium and – to a lesser extent – the sodium, concentrations of major elements are practically the same. The depletion of potas-

sium (and sodium) might be related to the hydrothermal fluids causing the tourmalinite formation and has been commonly referred to elsewhere (e.g. Bandyopadhyay et al., 1993; Slack et al., 1993; Slack, 1996; Torrez-Ruiz et al., 2003). An additional observation emphasizing the geochemical similarities of tourmalinites and phyllonites is their very similar chondrite-normalized REE pattern (Text-Fig. 6). However, the perfectly corresponding REE patterns of phyllonites, host rocks and tourmalinites strengthen the observation of Raith et al. (2004) that tourmalinites do not preferentially fractionate specific REEs or groups of REEs and, additionally, preclude a major change in the physicochemical conditions during tourmalinite formation. These observations suggest that the tourmalinites formed by in situ metasomatic alteration of meta-sediments, in the given case the precursors of the phyllites/phyllonites, by hydrothermal, boron-rich fluids.

A genetic interpretation of tourmalinites by hydrothermal replacement or, in other words, by boron metasomatism of psammopelitic rocks is supported by numerous authors e.g. Slack et al. (1993), Slack (1996), Torres-Ruiz et al. (2003) or Pesquera et al. (2005). However, this genetic model does not explain the primary source of the boron, namely, whether it is of magmatic origin or from the original meta-sedimentary rock pile.

As mentioned above, tourmalinite formation by diagenesis and metamorphism of B-rich evaporites – chemical sediments which may be enriched in iodine, bromine and chlorine – is one of the genetic models discussed in literature.

Though it is unlikely to expect a primary enrichment of these elements to survive a metamorphic overprint, it seemed to be worthwhile to analyse these elements (Tab. 2). As expected, concentrations of iodine and bromine of <0.5 ppm and chlorine around 20 ppm respectively are significantly below abundances in shales and schists (I: \approx 1 ppm; Br: 6 ppm and Cl: 200 ppm) as listed in Reimann & Caritat (1998) and are therefore of no relevance for further discussions.

Marine evaporites display higher $\delta^{11}\text{B}$ values compared to non-marine ones (Swihart et al., 1986; Barth, 1993; Jiang & Palmer, 1998; Frimmel & Jiang, 2001) enabling discrimination between these two possible precursor sedimentary environments. However, the average $\delta^{11}\text{B}$ value of \approx -11 ‰ of the tourmalinites investigated (Text-Fig. 7) precludes very clearly any relation to a marine evaporitic precursor environment (note the plain marine evaporitic origin of the tourmalinites published by Frimmel & Jiang, 2001 as plotted in Text-Fig. 7).

Average boron isotope concentrations of $\delta^{11}\text{B}$ of -11.2 ‰ and -11.3 ‰ for tourmalines from tourmalinites and a grobgness-hosted tourmaline veinlet (TU40) respectively (Tab. 4) are identical and would perfectly support the assumption of the grobgness to be the source of the boron. However, as $\delta^{11}\text{B}$ values cover a wide range in many geological environments (Text-Fig. 7) these $\delta^{11}\text{B}$ values are nevertheless not conclusive and do not necessarily preclude a sedimentary origin of the boron possibly inherited by re-melting of sediments.

With respect to the origin of boron and the formation of tourmalinites two possibilities have to be considered: a) the tourmalinite formation is contemporaneous with the intrusion of the granitic precursor of the grobgness. The granitic magma must therefore be assumed to be enriched in boron or b) the tourmalinites predate the granite intrusion in which case the source of boron necessary to form the tourmalinites remains unknown.

The first interpretation faces two difficulties: magmas specialized in boron are expected to be enriched in additional elements such as, e.g., tin, tungsten, lithium, beryllium or fluorine – just to mention a few. However, none of these elements is enriched in the tourmalinites to any significance as listed in Tab. 2a. Furthermore, the huge masses of grobgness within the phyllonites are in contradiction to the very limited size of single tourmalinite bodies displaying lateral extensions of some meters and thicknesses around 0.5 m only (see “Field Observations and Macroscopic Description”).

The second interpretation presumes the granitic precursor of the grobgness not to be associated with the tourmalinite formation. This granitic magma might be formed by re-melting of metasediments already hosting the tourmalinites or by migmatitization of sources not determinable anymore. The identical boron isotope compositions of tourmalinites and a tourmaline sample within the grobgness as mentioned do not contradict that interpretation as boron isotope ratios are controlled by the metamorphic protolith of derived magmas (Kasemann et al., 2000). Scarce tourmaline veinlets in the granite itself might be explained by internal magmatic fractionation or by an insignificant uptake of boron from sediments.

The lower $\delta^{11}\text{B}$ concentrations of -9.15 ‰ and -9.43 ‰ (samples TU17 and TU40; chapter “Boron Isotopic Composition”) respectively – if significant at all – cannot be explained at present and would need a regional investigation of boron isotopes in tourmalines.

The tourmalinites have been subject to the same kind of regional deformation and metamorphism that affected the whole Grobgness Complex. At least a twofold tectonic overprint as displayed by the phyllonitic host rocks can also be demonstrated in tourmalinites: clasts of tourmalinites imbedded in a fine grained tourmaline matrix (Text-Fig. 3c, d) point to the existence of tourmalinites prior to the youngest (latest) tectonic overprint. Additionally, this observation is strengthened by tourmaline individuals included in garnets (Text-Fig. 9) relating tourmaline formation to an older and garnet formation to a younger metamorphic event.

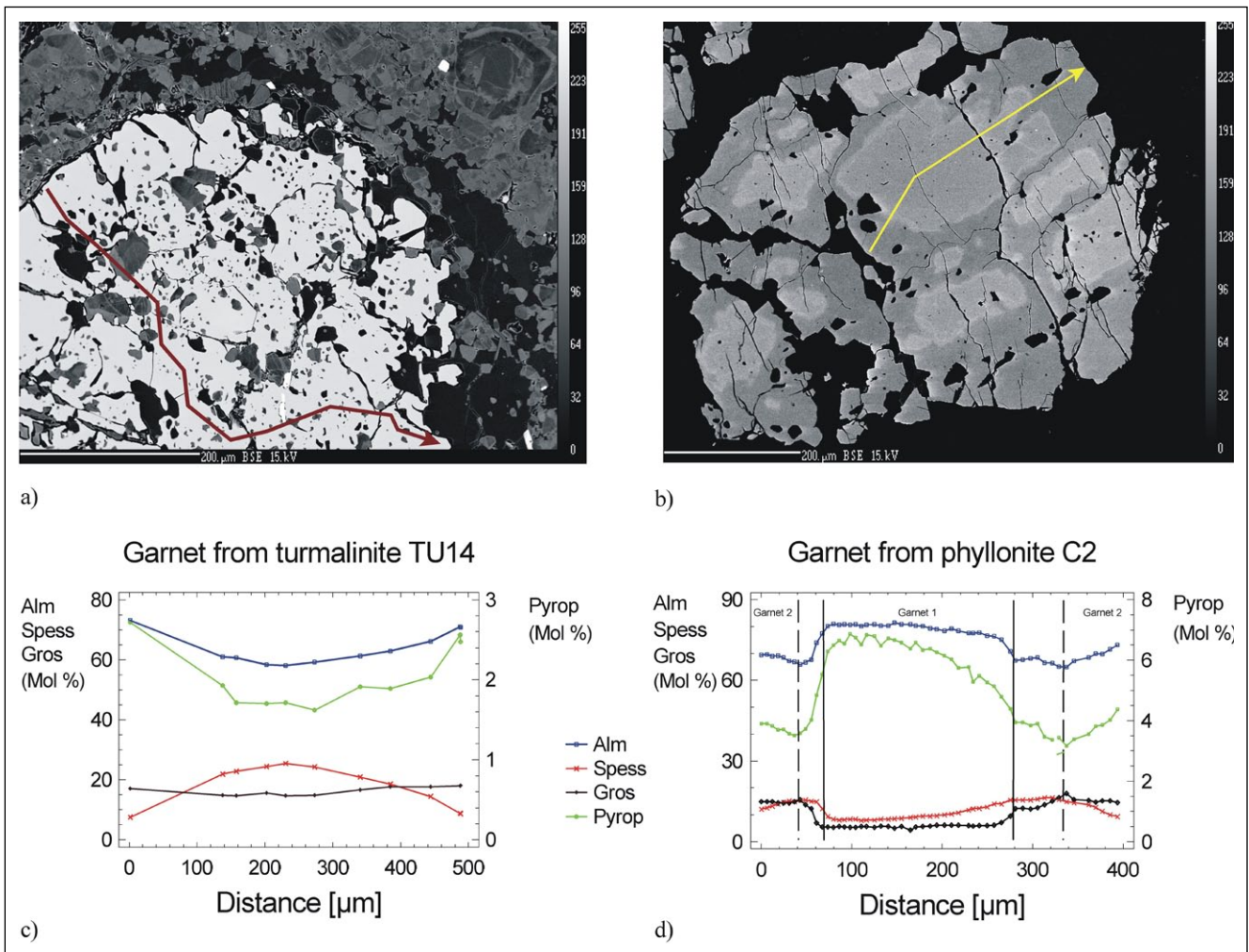
An additional argument in favour of a twofold metamorphic event is the zonal element distribution as observed in phyllonite hosted garnets (chapter “Garnets”, Text-Fig. 11). The formation of rims surrounding older cores is contemporaneous with the growth of garnets in tourmalinites.

Conclusions

Mineralogy and bulk chemistry of the tourmalinites investigated are simple and solely controlled by mutual relations of tourmaline and quartz respectively. Disregarding the elements boron and potassium, the bulk chemistries of tourmalinites and phyllonites are almost identical (Figs. 4b, 5). This favours strongly a tourmalinite genesis by in situ metasomatism of psammopelitic sediments caused by boron-rich hydrothermal fluids. The problem however is to determine the boron source, namely whether it is of granitic origin, i.e. from the granitic magma parental to the grobgness or derived from boron-rich (meta)sediments.

Marine sediments and clay minerals are known to be enriched in boron. However, a boron content of, e.g. for comparison, 2000 ppm which is the maximum boron content of clay minerals reported (Harder, 1970), would be equivalent to just about 5 wt.% tourmaline – insufficient to form tourmalinites as dealt with. It is therefore obvious that tourmalinite formation from sediments would necessarily need an additional external supply of boron. However, based on the boron isotope ratios at least a marine evaporitic origin of the tourmalinites could be excluded.

At a first sight, a derivation of the boron from the granitic magma parental to the grobgness seems to be reasonable due to the spatial vicinity of the tourmalinites and the grobgness, due to the tourmaline chemistry and finally due to the identical boron isotope values of tourmalines derived from tourmalinites and granite hosted tourmaline veinlets. However, this interpretation is neither in agreement with the striking imbalance between the huge masses of grobgness and the comparable tiny extensions of single tourmalinite bodies nor with the obvious lack of geochemical specialization of the tourmalinites not enriched in elements expected to be associated with boron-rich fluids expelled from a granitic magma. Finally, the identical boron isotope ratios of tourmalines from tourmalinites and



Text-Fig. 11a-d
 Zonal compositions of tourmalinite and phyllonite hosted garnets;
 a), b): analytical traverse;
 c) the zonal composition in the tourmalinite hosted garnet points to a continuous (“one-phase” growth);
 d) zonal composition of the phyllonite hosted garnet displays two garnet compositions; shape and zonality of the younger garnet – note in particular the right side of plot b) – corresponds to the tourmalinite hosted garnet in b);

from veinlets within the gneiss are ambiguous and by no means conclusive in so far as $\delta^{11}\text{B}$ ratios do not allow to discriminate between a granitic or sedimentary origin of boron respectively. A boron source related to the magma parental to the gneiss is therefore unlikely, or, in other words, the boron source for the tourmalinites remains unknown.

As pointed out (chapter “Geology”), the whole Grobneiss Complex – and therefore the tourmalinites – experienced Alpine metamorphism in greenschist facies giving rise to the diaphthoritic character of the metapelites and the mylonitization of the tourmalinites. This interpretation is mirrored by two garnet generations in the phyllonites with the younger phase (= garnet rims) contemporaneously grown with the tourmalinite hosted garnets the latter displaying inclusions of tourmaline individuals.

Summarizing all observations one can conclude that the tourmalinites predate the Upper Cretaceous metamorphic event and the magma parental to the gneiss as well.

Appendix

Analytical Methods

The following analytical procedures have been applied: ICP-emission spectroscopy for the major and ICP-MS for all of the trace elements; Na_2O_2 fusion combined with ICP for boron; fluorine by specific ion electrode and the halogens iodine, bromine and chlorine by NAA; all these analyses have been carried out by commercial laboratories. The boron isotope compositions were carried out at the “Geosciences and Georesources Institute of Italian National Research council laboratories” (IGG-CNR, Pisa) by S. Tonarini, Pisa; additional analytical details are given in Tonarini et al. (2003).

Microprobe analyses on garnets and tourmalines were conducted on a four-spectrometer CAMECA SX100 microprobe at the University of Vienna, Department of Lithospheric Research. Counts were obtained simultaneously from four spectrometers, using 15 keV accelerating voltage, a 1–2 μm beam diameter and a beam current of 20 nA. Natural and synthetic standards were used for calibrations and a PAP correction was applied to the data.

Acknowledgements

We thank the Austrian Academy of Sciences for financial support, in particular the chairman of the "Kommission für Grundlagen der Mineralrohstoffwirtschaft", em. Univ. Prof. Dr. H. Wagner; we thank Dr. F. Bernhard, Graz for field guidance, selected tourmalinite samples and sev-

eral chemical analyses of phyllonites; we thank ÖBB Infrastruktur AG – Dipl. Ing. J. Müller for permission to map and sample drill cores, we thank Dr. R. Schuster for allocating the geological map. We thank very cordially Prof. Zemann, Univ. of Vienna for numerous fruitful discussions and finally Mrs. Janine McKelson for improving the manuscript.

References

- Bandyopadhyay, B.K., Slack, J.F., Palmer, M.R. & Roy, A. (1990): Tourmalinites associated with stratabound and massive sulphide deposits in the Proterozoic Sakoli Group, Nagpur district, central India. – 8. IAGOD Symp., 867–885.
- Barth, S. (1993): Boron isotope variations in nature: a synthesis. – *Geol. Rundsch.*, **82**, 640–651.
- Bates, R.L. & Jackson, J.A. (Eds.) (1987): *Glossary of Geology*. – American Geological Institute, Alexandria, Virginia, 3rd edition.
- Benvenuti, M., Lattanzi, P. & Tanelli, G. (1989): Tourmalinite-Associated Pb-Zn-Ag Mineralization at Bottino, Apuane Alps, Italy: Geologic Setting, Mineral Textures and Sulfide Chemistry. – *Econ. Geol.*, **84**, 1277–1292.
- Bernhard, F. (2006): private archive, pers. comm.
- Chaussidon, M. & Albarede, F. (1992): Secular boron isotope variations in the continental crust: an ion microprobe study. – *Earth and Planetary Science Letters*, **108**, 229–241.
- De Capitani, L., Moroni, M. & Rodeghiero, F. (1999): Geological and geochemical characteristics of Permian tourmalinization at Val Trompa (southern Alps, northern Italy) and relationship with the Orobic tourmalinites. – *Periodico di Mineralogia*, **68**, 2, 185–212.
- Flügel, H.W. & Neubauer, F. (1984): Steiermark – Erläuterungen zur Geologischen Karte der Steiermark 1:200.000, Geol. B.-A., Wien.
- Frimmel, H.E. & Jiang, S.-Y. (2001): Marine evaporites from an oceanic island in the Neoproterozoic Adamastor ocean. – *Precamb. Research*, **105**, 57–71.
- Froitzheim, N., Plasienka, D. & Schuster, R. (2008): Alpine tectonics of the Alps and Western Carpathians. – In: McCann, T. (Ed.): *The geology of Central Europe. Volume 2: Mesozoic and Cenozoic*, Geol. Soc. London, 1141–1232.
- Göd, R. & Heiss, G. (2007): Geology, Mineralogy and Geochemistry of a Metapelite-Hosted Stratiform Arsenopyrite Mineralization (Pretul Alm, Austria). – *Jb. Geol. B.-A.*, **147/1-2**, 231–242.
- Göd, R. & Heiss, G. (2009): On the Geochemistry and Mineralogy of Phyllite Hosted Tourmalinites – Eastern Alps. – *Mitt. Österr. Miner. Ges.*, **155**, 61, Wien.
- Harder, H. (1970): Boron content of sediments as a tool in facies analysis. – *Sediment Geol.*, **4**, 153–175.
- Henry, D.J. & Guidotti, Ch.V. (1985): Tourmaline as a petrogenetic indicator mineral: an example from the staurolith-grade metapelites of NW Maine. – *Am. Mineralogist*, **70**, 1–15.
- Huber, M. (1994): Bildung und tektonische Bedeutung von Scherzonen (Leukophylliten) am Alpenostrand. – Unpubl. Diss., Montanuniversität Leoben, Leoben, 136 pp.
- Jiang, S.-Y. (2001): Boron Isotope geochemistry of hydrothermal ore deposits in china: a preliminary study. – *Phys. Chem. Earth (a)*, **26/9–10**, 851–858.
- Jiang, S.-Y. & Palmer, M.R. (1998): Boron isotope systematics of tourmaline from granites and pegmatites: a synthesis. – *Eur. J. Mineral.*, **10**, 1253–1265.
- Jiang, S.-Y., Palmer, M.R., Peng, Q.-M. & Yang, J.-H. (1997): Chemical and stable isotopic compositions of Proterozoic metamorphosed evaporates and associated tourmalines from the Houxianyu borate deposit, eastern Liaoning, China. – *Chem. Geol.*, **135/3-4**, 189–211.
- Jiang, S.-Y., Henry, D.H., de Brodtkorb, M.K. & Ametrano, S. (1999): Boron isotopes of tourmalines from the Sierras Pampaneas, Argentina. – In: Stanley, C.J. et al. (Eds.), *Mineral Deposits: Processes to Processing*, **1**. Proceedings of the 5th biennial SGA meeting and the 10th quadrennial IAGOD symposium, London 22–25 August 1999, 123–129, Balkema, Rotterdam
- Kasemann, S., Erzinger, J. & Franz, G. (2000): Boron recycling in the continental crust of the central Andes from the Palaeozoic to Mesozoic, NW Argentina. – *Contrib. Mineral. Petrol.*, **140**, 328–343.
- Mc Donough, W.F. & Sun, S.-S. (1995): The composition of the Earth. – *Chem. Geol.*, **120/3-4**, 223–253.
- Moreau, Ph. (1981): *Le Massif du Rabenwald (Autriche) et ses Mineralisations (Talc, Chlorite, Disthen, Leucophyllite)*. – Thèse, Univ. Franche-Comté Besançon, Fac. Sciences Techn., 327 pp, Besançon.
- Neubauer, F., Müller, W., Peindl, P., Moyschewitz, G., Wallbrecher, E. & Thöni, M. (1992): Evolution of Lower Austroalpine units along the eastern margins of the Alps: a review. – *ALPACA Field guide*, IGP/KFU, Graz, 97–114.
- Neubauer, F. & Frisch, W. (1993): The Austro-Alpine Metamorphic Basement East of the Tauern Window. – In: Raumer, J.F. v. & Neubauer, F. (Eds.): *Pre-Mesozoic Geology in the Alps*, 515–536, Springer-Verlag, Berlin – Heidelberg – New York.
- Palmer, M.R. & Swihart, G.H. (1996): Boron isotope geochemistry: an overview. – In: Grew, E.S. & Anowitz, L.M. (Eds.): *Boron: Mineralogy, petrology and geochemistry in the Earth's crust*, *Rev. Mineral.*, Mineralogical Society of America, Washington, **33**, 709–744.
- Pesquera, A. & Velasco, F. (1997): Mineralogy, geochemistry and geological significance of tourmaline-rich rocks from the Paleozoic Cinco Villas massif (western Pyrenees, Spain). – *Contributions to Mineralogy and Petrology*, **129**, 53–74.
- Pesquera, A., Torres-Ruiz, J., Gil-Crespo, P.P. & Jiang, S.-Y. (2005): Petrographic, Chemical and B-Isotopic Insights into the Origin of Tourmaline-Rich Rocks and Boron Recycling in the Martinamor Antiform (Central Iberian Zone, Salamanca, Spain). – *Journ. of Petrology*, **46**, 1013–1044.
- Prochaska, W., Bechtel, A. & Klötzli, U. (1992): Phyllonite Formation and Alteration of Gneisses in Shear Zones (Gleinalmkristallin, Eastern Alps/Austria). – *Mineral. Petrol.*, **45**, 195–216.
- Raith, J.G. (1988): Tourmaline Rocks Associated with Stratabound Scheelite Mineralization in the Austroalpine Crystalline Complex, Austria. – *Mineral. Petrol.*, **39**, 265–288.
- Raith, J.G., Riemer née Schöner, N. & Meisel, T. (2004): Boron metasomatism and behaviour of rare earth elements during formation of tourmaline rocks in the eastern Arunta Inlier, central Australia. – *Contrib. Mineral. Petrol.*, **147/1**, 91–109.
- Reimann, C. & Caritat, P. de (1998): *Chemical Elements in the Environment*. – 397 pp, Springer-Verlag, Berlin – Heidelberg – New York.
- Rockenschaub, M. (1991): Bericht 1990 über geologische Aufnahmen im Kristallin südlich von Müzzzuschlag auf Blatt Müzzzuschlag. – *Jb. Geol. B.-A.*, **134/3**, 492–493, Wien.
- Schafflechner, J. (2002): *Geologische und petrologische Aspekte am Ostrand des Grazer Paläozoikums (Naintsch)*. – Unpubl. Master's thesis, Karl-Franzens-Universität, 115 S., Graz.

- Schermaier, A., Haunschmid, B. & Finger, F. (1997): Distribution of Variscan I and S-type granites in the Eastern Alps: a possible clue to unravel pre-Alpine basement structures. – *Tectonophysics*, **272**, 315–333.
- Schuster, K., Berka, R., Draganits, E., Frank, W. & Schuster, R. (2001): Lithologien, Metamorphosegeschichte und tektonischer Bau der kristallinen Einheiten am Alpenostrand. – In: Mandl, G. (Ed.): Arbeitstagung 2001, Geol. B.-A., 29–56, Wien.
- Schuster, R., Koller, F., Hoeck, V., Hoinkes, G. & Bousquet, R. (2004): Metamorphic Evolution of the Eastern Alps. – In: Oberhänsli, R. (Ed.): *Metamorphic Structures of the Alps*, Mitt. Österr. Miner. Ges., **149**, 175–199, Wien.
- Schuster, R., Kallenberg, B. & Nowotny, A. (2008): Lower and Upper Austroalpine units at the eastern margin of the Eastern Alps (Burgenland, Lower Austria). – Unpubl. excursion guide, Geol. B.-A., 1–19, Wien.
- Slack, J.F. (1982): Tourmaline in Appalachian-Caledonian massive sulphide deposits and its exploration significance. – *Trans. Inst. Min. Metall.* **91** (B), B81–B89, London.
- Slack, J.F. (1996): Tourmaline associations with Hydrothermal Ore Deposits. – In: Grew, E.S. & Anowitz, L.M. (Eds.): *Boron – Mineralogy, Petrology and Geochemistry*, *Reviews in Mineralogy*, **33**, 559–643.
- Slack, J.F., Palmer, M.R., Stevens, B.P.J. & Barnes, R.G. (1993): Origin and Significance of Tourmaline-Rich Rocks in the Broken Hill District, Australia. – *Econ. Geol.* **88**, 505–541.
- Steven, N.M. & Moore, J.M. (1995): Tourmalinite Mineralization in the Late Proterozoic Kuiseb Formation of the Damara Orogen, Central Namibia: Evidence for a Replacement Origin. – *Econ. Geol.*, **90**, 1098–1117.
- Swihart, G.H., Moore, P.B. & Callis, E.L. (1986): Boron isotopic composition of marine and nonmarine evaporate borates. – *Geochim.Cosmochim. Acta*, **50**, 1297–1301.
- Tonarini, S., Pennisi, M., Adorni-Braccesi, A., Dini, A., Ferrara, G., Gonfiantini, R., Wiedenbeck, M. & Gröning, M. (2003): Inter-comparison of Boron Isotope and Concentration Measurements. Part I: Selection, Preparation and Homogeneity Tests of the Inter-comparison Materials. – *Geostandard Newsletters*, **27**, 21–39.
- Torres-Ruiz, J., Pesquera, A., Gil-Crespo, P.P. & Velilla, N. (2003): Origin and petrogenetic implications of tourmaline-rich rocks in the Sierra Nevada (Betic Cordillera, southeastern Spain). – *Chem. Geol.*, **197**, 55–86.
- Tourn, S.M., Herrmann, C.J., Amenetrana, S. & de Brodtkorb, M.K. (2004): Tourmalinites from the Eastern Sierras Pampeanas, Argentina. – *Ore Geology Reviews*, **24**, 229–240.
- Trumbull, R.B., Krienitz, M.-S., Gottesmann, B. & Wiedenbeck, M. (2008): Chemical and boron-isotope variations in tourmalines from an S-type granite and its source rocks: the Erongo granite and tourmalinites in the Damara Belt, Namibia. – *Contrib. Mineral. Petrol.*, **155**, 1–18
- Turekian, K.K. & Wedepohl, K.H. (1961): Distribution of the elements in some major units of the Earth's crust. – *Bull. Soc. Am.*, **72**, 175–191, Boulder, Colorado.
- Wedepohl, K.H. (1995): The composition of the continental crust. – *Geochim. Cosmochim. Acta*, **59**, 1217–1232.
- Wieseneder, H. (1961): Die Korund-Spinellfelse der Oststeiermark als Restite einer Anatexis. – *Joanneum, Min. Mittlgsbl.*, **1/1961**, Graz.
- Zhang, J.S., Passchier, C.W., Slack, J.F., Fliervoet, T.F. & de Boorder, H. (1994): Cryptocrystalline Permian Tourmalinites of possible Metasomatic Origin in the Orobic Alps, Northern Italy. – *Econ. Geol.*, **89**, 391–396.

Received: 24. February 2010, Accepted: 29. October 2010